

**Interactive comment on “Correction of real-time satellite precipitation with satellite soil moisture observations” by W. Zhan et al.**

**Anonymous Referee #2**

**Received and published: 10 July 2015**

*The manuscript presents a methodology to correct satellite-based precipitation estimates (TMPA-RT) using a land surface model (VIC) together with assimilation of soil moisture measurements from AMRS-E. This study follows a previous one published in RSE (Wanders et al. 2015) with basically the same co-authors. The paper topic is quite interesting and of interest for HESS. However, it has been really difficult for me to find the new contribution of this study compared to Wanders et al. 2015. Indeed, previous paper investigates various soil moisture sensors (AMSR-E, ASCAT, SMOS) as well as land surface temperatures to correct for precipitation estimates whereas the present paper only focuses on AMSR-E measurements. The only difference I found was related to the precipitation replicates generation which is based on percentiles instead of a random selection from a sampling area of  $1.75 \times 1.75$  around the selected location. Based on this, I would recommend the paper to be strongly re-written based on the following comments.*

---

We would like to thank Anonymous Referee #2 for these comments and suggestions, which will help us to produce an improved manuscript. Our response is provided below (in black) with original comments by Referee #2 quoted in blue italic font. Line numbers are marked according to the updated manuscript attached.

*1) As this paper follows a first study (with potential improvements), a clear reference to the Wanders et al. paper must be done as well as a comparison of the performance of the 2 methodologies. The manuscript should clearly state the originality/novelty of the present paper.*

---

Reviewer #1 also raised this issue. Below is our reply to Review #1 that addresses the concerns of Reviewer #2:

Novelties of our study compared to Wanders et al. (2015) include three aspects:

(1) Wanders et al. (2015) tried to overcome the limitations in 3 hourly satellite precipitation retrievals by correcting them using satellite soil moisture and land surface temperature (LST) observations. One important conclusion by Wanders et al. (2015) is that their results showed the limited potential for using satellite soil moisture observations for correcting precipitation if “all-weather” – i.e. microwave based – land surface temperatures are available coincidentally and at a high spatial resolution as was the case with AMSR-E.

But this isn’t always the case, and it is also noted that current low-frequency microwave soil moisture missions (specifically SMAP and SMOS) don’t have radiometers at frequencies useful for estimating land surface temperatures. (We recognize that a 37 GHz sensor is part of the AMSR2 system, the frequency used from AMSR-E, but the equatorial crossing time for AMSR2 is 7.5 hours out of phase with SMAP and SMOS.) In fact these missions use LST from weather models analysis fields in their algorithms. Unfortunately the lowest microwave frequency of AMSR2 precludes retrieving soil moisture from many areas with heavy vegetation, and data availability of AMSR2 is significantly less than AMSR-E, which is no longer operable. Another advantage of SMAP and SMOS over AMSR2 is the increased penetration depth of the observations. This reduces the impact of the saturation problem and hence improves their potential for correcting precipitation estimates. So improvements to satellite precipitation from the Global Precipitation Mission products can be achieved using algorithms and satellite soil moisture products from SMAP and SMOS. This is an important motivation for the study and this goal has been clarified in the revision. (See lines 82-121). Thus, in our study, we focus exclusively on the usefulness of assimilating soil moisture products to improve satellite rainfall.

(2) We present in the paper improvements in the generation of rain particles and the bias-correction of the satellite soil moisture observations, as well as enhancements to the assimilation algorithm to maximize the information that

can be gained from using soil moisture alone in adjusting precipitation. Due to the very strong and complicated spatial structure of precipitation, that is non-Gaussian and non-stationary in both time and space, a more advanced method is applied to generate possible precipitation fields than used or presented in earlier studies or in Wanders et al., (2015). Furthermore, a more advanced bias correction method is also applied to account for the reported problems (Wanders et al., 2015) in the second order statistics of the soil moisture retrievals (This has been clarified in [line 123-139](#))

(3) Wanders et al. (2015) and previous studies are based on the assumption that the SM retrievals are 100% accurate and contain no errors. We evaluated this assumption by analyzing the impact of uncertainties associated with the soil moisture retrievals (added in [line 677-681](#)).

A new section has been added with detailed inter-comparisons with the current work. Please see Section 5 of the revised paper ([line 576-685](#)) for a more detailed description between our study and Wanders et al. (2015, [line 686-750](#)), including a quantitative comparison ([line 709-750](#)). Regarding comparisons to the earlier studies, we summarized previous finding and our novelties in [line 577-685](#).

---

*2) Globally, there are too much figures and, in most of them, the legend is not clear enough to understand the figures. (cf Fig. 2, 4, 6, 7)*

---

We appreciate the comment to reduce the number of figures in the text. We removed Figure 5, 10, 15, & 16; combined Figure 7 & 8 (now [Figure 6](#)); updated Figure 9 (now [Figure 7](#)), Figure 11 & 13 (now [Figure 9 & 10](#)) and Figure 14 (now [Figure 11](#)); added (now) [Figure 12 & 13](#) with a revised structure of the analysis in Section 4 of the manuscript. Please see the revised paper for a more in-depth analysis of our results (particularly the material between [lines 478 and 575](#)).

---

*3) Figure 5 is useless as it is obvious that after assimilation of AMSR-E into VIC the difference between VIC and AMSR-E should be smaller. Instead of Fig. 5, it would be better to get a temporal graph showing (in one pixel) how the VIC soil moisture simulation is modified after AMSR-E simulation and, how the TMPA-RT precipitation rate is modified.*

---

Figure 5 has been removed. The suggestion of a temporal graph of a single pixel is indeed a better way showing the effectiveness of adopted method. However, given that the assimilation was done for a 5-year period (2003-2007) (~1,700 time steps) at 0.25-degree resolution over CONUS (~17,000 grids), it is difficult to show meaningful time series. Selective periods can show either fantastic or terrible results. Thus, we feel the spatial examples in (now) [Figure 5 & 8](#) with boxplots in (now) [Figure 6 & 11](#) are sufficient to illustrate the performance of the algorithm.

---

*Previous paper (Wanders et al.) used quite interesting metrics to assess precipitation estimates (POD, FAR) whereas this one disregards these scores without any explanation.*

---

Categorical statistics (POD, FAR) have been added ([Figure 12](#)) and discussed in the revised paper ([line 478-526](#)).

# Correction of real-time satellite precipitation with satellite soil moisture observations

Wang Zhan<sup>1</sup>, Ming Pan<sup>1</sup>, Niko Wanders<sup>1,2</sup>, Eric F. Wood<sup>1</sup>

[1] Department of Civil and Environmental Engineering, Princeton University, Princeton, NJ, USA

[2] Department of Physical Geography, Utrecht University, Utrecht, the Netherland

## Abstract

Rainfall and soil moisture are two key elements in modeling the interactions between the land surface and the atmosphere. Accurate and high-resolution real-time precipitation is crucial for monitoring and predicting the on-set of floods, and allows for alert and warning before the impact becomes a disaster. Assimilation of remote sensing data into a flood-forecasting model has the potential to improve monitoring accuracy. Space-borne microwave observations are especially interesting because of their sensitivity to surface soil moisture and its change. In this study, we assimilate satellite soil moisture retrievals using the Variable Infiltration Capacity (VIC) land surface model, and a dynamic assimilation technique, a particle filter, to adjust the Tropical Rainfall Measuring Mission Multi-satellite Precipitation Analysis (TMPA) real-time precipitation estimates. We compare updated precipitation with real-time precipitation before and after adjustment and with NLDAS gauge-radar observations. Results show that satellite soil moisture retrievals provide additional information by correcting errors in rainfall bias. The assimilation is most effective in the correction of medium rainfall under dry to normal surface condition; while limited/negative improvement is seen over wet/saturated surfaces. On the other hand, high frequency noises in satellite soil moisture impact the assimilation by increasing rainfall frequency. The noise causes larger uncertainty in the

Authors 8/31/2015 3:38 PM

Deleted: Wanders<sup>2</sup>

Authors 8/31/2015 3:38 PM

Deleted: High accuracy soil moisture retrievals, when merged with precipitation, generally increase both rainfall frequency and intensity, and are

Authors 8/31/2015 3:38 PM

Deleted: Errors from soil moisture, mixed among

Authors 8/31/2015 3:38 PM

Deleted: real signal, may generate a

false-alarmed rainfall over wet regions. A threshold of 2 mm/day soil moisture change is identified and applied to the assimilation, which masked out most of the noise.

Authors 8/31/2015 3:38 PM

**Deleted:** signal approximately 2mm

Authors 8/31/2015 3:38 PM

**Deleted:** and thus lower the precipitation accuracy after adjustment.

## 1 Introduction

Precipitation is perhaps the most important variable in controlling energy and mass fluxes that dominate climate and particularly the terrestrial hydrological and ecological systems. Precipitation estimates, together with hydrologic models, provide the foundation for understanding the global energy and water cycles (Sorooshian, 2004; Ebert et al., 2007). However, obtaining accurate measurements of precipitation at regional to global scales has always been challenging due to its small-scale, space-time variability, and the sparse networks in many regions. Such limitations impede precise modeling of the hydrologic responses to precipitation. There is a clear need for improved, spatially distributed precipitation estimates to support hydrological modeling applications.

In recent years, remotely sensed satellite precipitation has become a critical data source for a variety of hydrological applications, especially in poorly monitored regions such as sub-Saharan Africa due to its large spatial coverage. To date, a number of fine-scale, satellite-based precipitation estimates are now in operational production. One of the most frequently used is the Tropical Rainfall Measuring Mission Multi-satellite Precipitation Analysis (TMPA) product (Huffman et al., 2007). Over the 17 years lifetime since the launch of the Tropical Rainfall Measuring Mission (TRMM) in 1997, a series of high resolution (0.25-degree and 3-hourly), quasi-global (50°S - 50°N), near-realtime, TRMM-based precipitation estimates have been developed and made available to the research and applications communities (Huffman et al., 2007; 2010). Flood forecasting and monitoring is one major application for real time satellite rainfall products (Wu et al, 2014). However, the applicability of satellite precipitation products for near real-time hydrological applications that include drought and flood monitoring has been hampered by their need for gauge-based adjustment.

While it is possible to create such estimates solely from one type of sensor, researchers have increasingly moved to using combinations of sensors in an attempt to improve accuracy, coverage and resolution. A promising avenue for rainfall correction is through the assimilation of satellite-based surface soil moisture into a water balance model (Pan and Wood, 2006). Over land, the physical relationship between variations in soil water storage and rainfall accumulation contain complementary information that can be exploited for the mutual benefit of both types of products (Massari et al., 2014; Crow et al., 2009). Unlike instantaneous rain rate, satellite surface soil moisture retrievals utilize low frequency microwave signals and possess some memory reflecting antecedent rainfall amounts.

Studies have demonstrated that in situ (Brocca et al., 2009, 2013; Matgen et al., 2012) and satellite (Francois et al., 2003; Pellarin et al., 2008, 2013; Brocca et al., 2014) estimates of surface soil moisture could contribute to precipitation estimates by providing useful information concerning the sign and magnitude of antecedent rainfall accumulation errors. In particular, Brocca et al. (2014) estimated daily rainfall on a global scale based on satellite SM products by inverting the soil water balance equation. Crow et al. (2003, 2009, 2011) corrected space-borne rainfall retrievals by assimilating remotely sensed surface soil moisture retrievals into an Antecedent Precipitation Index (API) based soil water balance model using a Kalman filter (Kalman, 1960). However, these studies focused on multi-day aggregation periods and a space aggregated correction at 1° resolution for the corrected precipitation totals. This limits their applicability in applications such as near real-time flood forecasting. Wanders et al. (2015) tried to overcome this limitation by the correction of 3 hourly satellite precipitation totals with a set of satellite soil moisture and land surface temperature observations. One important conclusion by Wanders et al. (2015) is that their results showed the limited potential for satellite soil moisture observations for correcting precipitation if “all-weather” – i.e. microwave based – land surface temperatures are available coincidently and at high spatial resolution as was the case with AMSR-E.

But this isn’t always the case, and it is also noted that current low-frequency microwave soil moisture missions (specifically SMAP and SMOS) don’t have radiometers at

Authors 8/31/2015 3:38 PM

**Deleted:** spaceborne

Authors 8/31/2015 3:38 PM

**Deleted:** a simple

Authors 8/31/2015 3:38 PM

**Deleted:** The hydrologic response

Authors 8/31/2015 3:38 PM

**Deleted:** to precipitation is especially

Authors 8/31/2015 3:38 PM

**Deleted:** in

Authors 8/31/2015 3:38 PM

**Deleted:** an explicit and sophisticated physical model is needed to accurately recover

Authors 8/31/2015 3:38 PM

**Deleted:** information about the rainfall more precisely, e.g. wetted area. This is because most storm systems have a very strong and complicated spatial structure that is non-Gaussian and non-stationary in both time and space (Wanders et al., 2015).

Authors 8/31/2015 3:38 PM

**Deleted:** In this paper we present a method to improve real-time remote sensing precipitation products by merging retrievals with soil moisture remote sensing products through a Particle Filter (PF),

frequencies useful for estimating land surface temperatures, even though a 37 GHz sensor is part of the AMSR2 system. In fact SMAP and ECMWF/SMOS use LST from weather models analysis fields in their algorithms. Unfortunately the lowest microwave frequency of AMSR2 precludes retrieving soil moisture from many areas with heavy vegetation, and data availability of AMSR2 is significantly less than AMSR-E, but is no longer operable. So improvements to satellite precipitation from the Global Precipitation Mission products must rely solely on satellite soil moisture products from SMAP and SMOS, and the improvements to the assimilation algorithms is the goal of this study.

Thus, we focus exclusively on the usefulness of assimilating soil moisture products to improve satellite rainfall. We propose as part of the work how to improve the generation of rain particles and the bias-correction of the satellite soil moisture observations, as well as to enhance the assimilation algorithm to maximize the information that can be gained from using soil moisture alone to adjust precipitation. Due to the very strong and complicated spatial structure of precipitation, that is non-Gaussian and non-stationary in both time and space (Wanders et al., 2015), a more advanced method is applied to generate possible precipitation fields than were used in earlier studies or in Wanders et al. (2015) (see section 2.2.2). Furthermore, a more advanced bias correction method is also applied to account for the reported problems in the second order statistics of the soil moisture retrievals. We used a soil moisture remote sensing product to improve real-time remote sensing precipitation product, TMPA 3B42RT, through a Particle Filter (PF) and therefore offer an improved basis for quantitatively monitoring and predicting flood events, especially in those parts of the world where in-situ networks are too sparse to support more traditional methods of hydrologic monitoring and prediction. The precipitation enhancement experiments are carried out over the continental U.S. (CONUS) and the precipitation skill is validated against the NLDAS gauge-radar precipitation product. Section 5 presents a comparison of the results from this study to the earlier studies related to improving satellite precipitation.

## 2 Methods

### 2.1 Overview

Random replicates of satellite precipitation are generated based on real-time TMPA (3B42RT) retrievals and its uncertainty (Pan et al., 2010), which are then used to force the VIC land surface model (LSM) where one output of interest is surface soil moisture. Satellite soil moisture data products are compared and merged with the 3B42RT product to improve the accuracy of the satellite precipitation estimates. A schematic for the study approach is provided in Figure 1. Based on real-time 3B42RT retrievals, a set of possible precipitation estimates (a.k.a. replicates or particles)  $\{p^i\}_{i=1,2,\dots,N}$  is generated with assigned initial prior probability weights  $\{w^i\}_{i=1,2,\dots,N}$ . These rainfall rates are then used to force the VIC land surface model to produce soil moisture predictions  $\{\theta^i\}_{i=1,2,\dots,N}$ . Retrievals of AMSR-E satellite surface soil moisture using the Land Surface Microwave Model (LSMEM) (Pan et al., 2014) are then merged with the LSM-based soil moisture within the Particle Filter (PF) that compares AMSR-E/LSMEM changes in soil moisture,  $\Delta SM$ , to the LSM predicted soil moisture changes. From these, posterior weights  $\{w^{i+}\}_{i=1,2,\dots,N}$  are calculated for each precipitation member (particle) that takes into account the uncertainties of AMSR-E/LSMEM  $\Delta SM$  retrievals. From these updated weights, an updated precipitation probability distribution is constructed, where the precipitation particle with highest probability is taken as the “best” adjusted precipitation estimate (3B42RT<sub>ADJ</sub>). The procedure is carried out over the continental US (CONUS) region on a grid-by-grid basis (0.25-degree) and a daily time step. Allowing for 6 months model spin-up period, the adjustment is done from January 2003 to July 2007.

### 2.2 Modeling, Statistical Tools and Data Sources

#### 2.2.1 The Particle Filter

Data assimilation methods are capable of dynamically merging predictions from a state equation (i.e. the land surface model) with measurements (i.e. AMSR-E retrievals) to minimize uncertainties from both the predictions and measurements. It is assumed that

the source of uncertainty in the land surface model predictions come solely from the real-time satellite precipitation, so that the particle filter (PF) provides an algorithm to update the precipitation based on the AMSR-E retrievals. The state evolution of a particle filter from discrete time  $t-1$  to  $t$  can be represented as:

$$\theta_t = f_t(\theta_{t-1}, p_t, \kappa_t, \alpha_t) \quad (1)$$

where  $\theta_t$  is the 1<sup>st</sup> layer soil moisture at time  $t$ , whose value is predicted by the state equation Eq.(1) as  $f_t(\bullet)$ , and in the study is the hydrological model VIC, which takes in forcing data, including precipitation ( $p_t$ ) and other forcings ( $\kappa_t$ ); and simulates land surface states (soil moisture and soil temperatures at various levels, snow, etc.) and fluxes (evapotranspiration, runoff) at time  $t$ . Herein we are basically interested only in the 1<sup>st</sup> layer (top 10cm) soil moisture state and precipitation forcing, so other states and fluxes are not explicitly shown.  $\alpha_t$  is the random error in the prediction of  $\theta_t$ , whose statistics are known but not its value at any specific time.

At time  $t$ , the satellite surface soil moisture retrieval,  $\theta_t^*$ , can be related to the VIC modeled 1<sup>st</sup> layer soil moisture  $\theta_t$  as:

$$\theta_t^* = h_t(\theta_t, \beta_t) \quad (2)$$

where  $h_t$  is taken as a regression that transforms the VIC simulated 1<sup>st</sup> layer soil moisture to satellite surface soil moisture.  $\beta_t$  is the noise in this regression relationship. The two noises  $\alpha_t$  and  $\beta_t$  are assumed to be independent of each other at all times  $t$ .

At time  $t$ , given a 3B42RT precipitation estimate,  $p_t^{\text{sat}}$ , a set of  $N$  precipitation replicates  $\{p_t^i\}_{i=1,2,\dots,N}$  and their associated initial prior probability weight  $\{w_t^i\}_{i=1,2,\dots,N}$  are generated.

$$g(p_t^{\text{sat}}) \sim \{p_t^i, w_t^i\}_{i=1,2,\dots,N} \quad (3)$$

$$\sum_{i=1}^N w_t^i = 1 \quad (4)$$

$g(\cdot)$  is a probability density function. For  $N$  precipitation replicates,  $\{p_t^i\}_{i=1,2,\dots,N}$ , the propagation of the states from time step  $(t-1)$  to  $t$  is by the VIC land surface model



194 represented in Eq.(1). The VIC land surface model simulates the 10cm 1<sup>st</sup> layer soil  
 195 moisture,  $\{\theta_t^i\}_{i=1,2,\dots,N}$  for each precipitation replicate.

$$196 \quad \{\theta_t^i = f_t(\theta_{t-1}, p_t^i, \kappa_t, \alpha_t)\}_{i=1,2,\dots,N} \quad (5)$$

197 with the associated weights assigned to the precipitation member:

$$198 \quad \{\theta_t^i, w_t^i\}_{i=1,2,\dots,N} = \{f_t(\theta_{t-1}, p_t^i, \kappa_t, \alpha_t), w_t^i\}_{i=1,2,\dots,N} \quad (6)$$

199 If the satellite soil moisture retrieval at time  $t$  is  $\theta_t^*$ , the update of precipitation forcing is  
 200 accomplished by updating the importance weight of each replicate given the  
 201 “measurement”  $\theta_t^*$ :

$$202 \quad w_t^{i+} \sim \{g(\theta_t^i | \theta_t^*)\}_{i=1,2,\dots,N} \quad (7)$$

$$203 \quad \sum_{i=1}^N w_t^{i+} = 1 \quad (8)$$

204 The likelihood function  $g(\theta_t^i | \theta_t^*)$  can be derived from  $h_t$  and  $g(\beta_t)$ . The schematic of the  
 205 utilized strategy is shown in Figure 2. The primary disadvantage of the particle filter is  
 206 the large number of replicates required to accurately represent the conditional probability  
 207 densities of  $p_t$  and  $\theta_t$ . When the measurements exceed a few hundred, the particle filter is  
 208 not computationally practical for land surface problems. Considering computation  
 209 efficiency, we set the number of independent particles,  $N$ , from the prior distribution to  
 210 be 200.

## 211 **2.2.2 Precipitation Replicates Generation**

212 We generate precipitation replicates,  $\{p_t^i\}_{i=1,2,\dots,N}$ , based on statistics comparing NLDAS  
 213 and 3B42RT precipitation, as shown in Figure 3. Given a 3B42RT precipitation  
 214 measurement (binned by magnitude), with bin minimum and maximum indicated in  
 215 Figure 3, precipitation replicates are generated based on the corresponding 15<sup>th</sup>, 30<sup>th</sup>, 70<sup>th</sup>,  
 216 85<sup>th</sup> percentiles and the maximum NLDAS precipitation of the particular quantile bin as  
 217 follows: 15% of the replicates are generated with values uniformly distributed from 0 and  
 218 15<sup>th</sup> percentile; 15% of replicates with values from 15<sup>th</sup> to 30<sup>th</sup> percentile; 20% of  
 219 replicates with values from 30<sup>th</sup> percentile to the median; 20% of the replicates generated  
 220 from the median to 70<sup>th</sup> ; 15% with values from 70<sup>th</sup> to 85<sup>th</sup> percentile; and 15% from the

85<sup>th</sup> percentile to the maximum precipitation value. Note that although the generation of particles is based on statistics calculated from NLDAS, results show little difference generating precipitation ensembles uniformly distributed between 0 and 200 mm/day.

### 2.2.3 AMSR-E/LSMEM Soil Moisture Retrievals

The soil moisture product is derived from multiple microwave channels of the Advanced Microwave Scanning Radiometer for EOS (AMSR-E) instrument. The retrieval algorithm by Pan et al. (2014) is an enhanced version of the Land Surface Microwave Emission Model (LSMEM). The near surface soil moisture and vegetation optical depth (VOD) are estimated simultaneously from a dual polarization approach that utilizes both horizontal (H) and vertical (V) polarizations measurement by the space-borne sensor. The input AMSR-E brightness temperature comes from the NSIDC AMSR-E/Aqua Daily Global Quarter-Degree Gridded Brightness Temperatures product (overlapping swaths in the same day are truncated so that only the latest one is present). Consequently, the soil moisture retrievals are also gridded at 0.25-degree with one ascending map and one descending map at the daily time step. A maximum threshold value of 0.6 m<sup>3</sup>/m<sup>3</sup> has been applied manually to reduce error from open water bodies. According to Pan et al. (2014), the soil moisture dataset based on observations from AMSR-E are shown to be consistent at large scales in terms of reproducing the spatial pattern of soil moisture from VIC land surface model simulation. Ascending soil moisture retrievals (equatorial crossing time 1:30PM local time) is assimilated in this study.

Similarly, while the spatial patterns of the basic statistics of AMSR-E/LSMEM SM retrievals compare well to VIC simulations (Pan et al., 2014), VIC has its top layer (10 cm), which is deeper than the detection depth of AMSR-E, so that the mean and temporal variability of the retrievals are higher than the VIC simulated soil moisture (Figure 4 in Pan et al., 2014). Considering this difference between detection depths, we pre-process soil moisture retrievals as follows:

1) Rescale soil moisture retrievals (AMSR-E/LSMEM SM) to have the same minimum and maximum range as VIC simulated 1<sup>st</sup> layer soil moisture.

Authors 8/31/2015 3:38 PM

Deleted: 200mm

2) Calculate a daily soil moisture change. As satellite retrievals are manually truncated to be no more than  $0.6 \text{ m}^3/\text{m}^3$  (equivalent to 60mm of water in the top soil layer in VIC), retrievals larger than  $0.6 \text{ m}^3/\text{m}^3$  are excluded.

3) Fit a 2<sup>nd</sup> order polynomial regression model with  $\Delta\text{SM}$  (all units in mm of water in the top layer) from satellite and VIC simulation on a monthly basis and  $3\times 3$  grid scale (window).

After pre-processing, the distribution of soil moisture change matches fairly well with  $\Delta\text{SM}_{\text{VIC}}$  (Figure 4). The mean absolute difference reduces from a spatial average of 5.25 mm/day to 0.71 mm/day, with relatively larger value over eastern CONUS. According to Pan et al. (2014), the no-skill or negative-skill areas occur mostly over eastern dense forests due to vegetation blockage of the soil moisture signal (Pan et al., 2014). The accuracy of soil moisture retrievals is also limited by mountainous topography and the occurrence of snow and frozen ground during winter whose identification from satellite observations is often difficult. For the purpose of this study, we assign zero weight to the  $3\text{B42RT}_{\text{ADJ}}$  and rely exclusively on the initial 3B42RT precipitation for time steps when the VIC model predicts snow cover or frozen surfaces.

#### **2.2.4 VIC Land Surface Model**

The Variable Infiltration Capacity (VIC) model (Liang et al., 1994; Gao et al., 2010) is used to dynamically simulate the hydrological responses of soil moisture to precipitation, surface radiation and surface meteorology. The VIC model solves the full energy and water balance over each 0.25-degree-grid-cell independently, thus ensuring its computational efficiency. The assumption of independency poses limitation on the application of LSM at very high spatial resolution (e.g.  $1\text{km}\times 1\text{km}$ ) over large areas. Three-layer-soil-moisture is simulated through a soil-vegetation-atmosphere transfer (SVAT) scheme, which also accounts for sub-grid scale heterogeneity of vegetation, soil and topography. A detailed soil moisture algorithm description can be found in Liang et al. (1996). The VIC model has been validated extensively over CONUS by evaluating soil moisture and simulations to observations (Robock et al., 2003; Schaake et al., 2004).

### 3 Idealized Experiment

Before applying the Particle Filter assimilation algorithm on 3B42RT precipitation estimates, we conducted an idealized experiment where we treat the NLDAS precipitation as the “truth” and the NLDAS precipitation forced VIC simulations as “satellite observed” soil moisture. As an idealized experiment, we adjust TMPA real-time precipitation estimates based on these “satellite observations”. Phase 2 of the North American Land Data Assimilation System (NLDAS-2) rainfall forcing combines hourly WSR-88D radar analyses from the National Weather Service (NWS) and daily gauge reports (~13,000/day) from the Climate Prediction Center (CPC) (Ek et al., 2011). The dataset, with a spatial resolution of 0.125 degree and hourly observations, was pre-processed into 0.25-degree daily precipitation to be consistent with that of 3B42RT and AMSR-E/LSMEM SM datasets. Hourly NLDAS and 3-hourly 3B42RT precipitation is aggregated into daily precipitation defined by a period shifted ~7.5 hours into the future (9:00PM-9:00PM), allowing for a necessary delay for soil moisture to respond to incoming rainfall. The idealized experiment is designed to test whether the algorithm is able to retrieve rainfall forcing with soil moisture change, assuming that the soil moisture observations are 100% accurate.

Results show that, with the knowledge of 1<sup>st</sup> layer soil moisture change (via the “satellite observations”), the adjustment is able to recover intensity and spatial pattern of forcing precipitation (Figure 5g). Average mean absolute error (MAE) of daily rainfall amount is reduced by 52.9% (2.91 mm/day to 1.37 mm/day) over the region. Figure 5a to Figure 5e shows an example of the recovered rainfall field from the idealized experiment for 27<sup>th</sup> Oct. 2003. The spatial pattern matches the original NLDAS precipitation well.

#### 3.1 Effect of surface soil saturation

While successfully recovering the general pattern of NLDAS precipitation based on first layer soil moisture, the idealized experiment is not always able to recover the precipitation volume due to the fact that the top layer soil moisture alone does not contain the complete memory of the previous day’s rainfall. Deeper soil moisture, evapotranspiration and runoff also carry part of this information. As the surface gets

Authors 8/31/2015 3:38 PM

Deleted: Figure 6).

Authors 8/31/2015 3:38 PM

Deleted: 91mm

Authors 8/31/2015 3:38 PM

Deleted: 37mm

wetter, the VIC 1<sup>st</sup> layer soil moisture has smaller variation. If the incoming precipitation brings the surface to saturation, the VIC model redistributes the soil moisture vertically through vertical moisture flow and generates runoff. Hence soil moisture increments,  $\Delta SM$ , near saturation are less correlated with incoming precipitation as they change minimally to additional incoming rainfall. An example demonstrating this saturation effect is shown in Figure 5f to Figure 5j. When incoming precipitation brings the surface SM to (near) saturation, there is very limited improvement after the adjustment. Because of the low sensitivity of the soil surface to precipitation, there is little change in  $\Delta SM$  in response to precipitation variations among the replicates. It is almost always the case that the algorithm is not able to find a “matching”  $\Delta SM$ .

We separately evaluate the skill improvement in the recovered NLDAS precipitation with and without surface saturation. Figure 6 confirms the effect of surface saturation on adjusted precipitation, which is well described in previous studies (e.g. Brocca et al., 2013, 2014). The recovered precipitation, when the surface soil is saturated, only contributes more noise rather than an improvement to the rainfall estimates. The VIC model computes the moisture flow between soil layers using an hourly time step. If the 1<sup>st</sup> layer soil moisture exceeds its maximum capacity, it is considered to be a surface saturation case. As seen in Figure 5, there is very limited or negative skill in the recovered precipitation under saturated surface soil moisture conditions. Such circumstances are identified and the AMSR-E/LSMEM  $\Delta SM$  observation disregarded by assigning zero weight to the  $3B42RT_{ADJ}$  values. Thus for wetter areas with heavy precipitation that potentially would bring the surface soil moisture to saturation, the 3B42RT product is less likely to be adjusted according to satellite  $\Delta SM$  and the best precipitation estimate is 3B42RT.

### 3.2 Effect of SM uncertainty

In the idealized experiment, NLDAS-VIC soil moisture is taken as truth with zero uncertainty associated with  $(\theta_t^*)$ . However, this assumption is not valid for real satellite SM retrievals, mean absolute error of which is approximately 3% vol./vol. (McCabe et al., 2005). To consider this, we added error to the “truth” SM (normally distributed with zero mean and standard deviations of 1mm, 2mm, 3mm, 4mm and 5mm), and simulated

Authors 8/31/2015 3:38 PM  
Moved (insertion) [1]

Authors 8/31/2015 3:38 PM  
Deleted: (Figure 6).

Authors 8/31/2015 3:38 PM  
Deleted: 0.

Authors 8/31/2015 3:38 PM  
Deleted: , 1.0mm, 1.5mm, 2.0mm, 2.5mm, 3.0mm, 3.5mm, 4.0mm 4.5mm and 5.0mm

344 the effect of SM uncertainty to evaluate the associated adjustment errors. Figure 7 shows  
 345 that larger soil moisture observation errors lead to larger error variation after adjustment.  
 346 This also suggests that soil moisture responds to precipitation non-linearly based on  
 347 different initial conditions. An estimated wetter surface has lower sensitivity to an  
 348 incoming rainfall amount, resulting in larger error in the recovered NLDAS precipitation.  
 349 As shown in Figure 7, the error standard deviation of the recovered NLDAS precipitation  
 350 increases with surface water content (statistics shown in Table 2). As we add noise larger  
 351 than  $N(0, 1\text{mm})$  into “true” SM observation, there is a wet bias of approximately  $1$   
 352  $\text{mm/day}$  regardless of 1<sup>st</sup> layer soil moisture level. This suggests that when the difference  
 353 between 1<sup>st</sup> layer SM and saturation is less than  $8\text{ mm}$ , the median of the errors in the  
 354 recovered NLDAS precipitation grows from  $0.16\text{ mm/day}$  to  $1.89\text{ mm/day}$  when we add  
 355  $N(0, 5\text{mm})$  noise, while inter-quantile range (IQR) increases from  $1.71\text{ mm/day}$  to  $7.04$   
 356  $\text{mm/day}$ . Acknowledging such a wet bias, to avoid introducing any more unintentional  
 357 bias in the  $3B42RT_{ADJ}$  estimates, we take as zero the uncertainty of AMSR-E/LSMEM  
 358 SM retrievals, i.e. we take  $h_t(\theta_t)$  as our single observation  $\theta_t^*$  and adjust the  $3B42RT$   
 359 estimates accordingly.

360 It is noteworthy that the soil moisture change is calculated based on previous days’ soil  
 361 water contents. Therefore errors tend to accumulate over time until they are “re-set” when  
 362 a significant precipitation event takes place. This type of uncertainty accounts for a small  
 363 portion of the total error in the adjusted precipitation (black being the no error case in  
 364 Figure 7 with the “true” change in soil moisture from every time step). As complete  
 365 global coverage is not provided with each orbit of the AMSR-E sensor, on average 44.01%  
 366 of the time steps ( $<0.6\text{ m}^3/\text{m}^3$ ) during the study period have observations, with more  
 367 frequent overpasses at higher latitudes (Figure 4e in Pan et al., 2014). This observation  
 368 gap unavoidably introduces extra uncertainty in the retrieval of the precipitation signal.  
 369 To further avoid possible additional errors, we update the forcing rainfall when a  $\Delta\text{SM}$   
 370 temporal match ( $\pm 0.4\text{mm}$ ) is available, and keep the original precipitation if a match isn’t  
 371 available.

Authors 8/31/2015 3:38 PM

Deleted: 0.5mm

Authors 8/31/2015 3:38 PM

Deleted: 1mm

Authors 8/31/2015 3:38 PM

Deleted: 8mm

Authors 8/31/2015 3:38 PM

Deleted: 16mm

Authors 8/31/2015 3:38 PM

Deleted: 89mm

Authors 8/31/2015 3:38 PM

Deleted: 5.0mm

Authors 8/31/2015 3:38 PM

Deleted: 71mm

Authors 8/31/2015 3:38 PM

Deleted: 04mm

#### 4 Improvement on real-time precipitation estimates and their validation

The adjustment of real TMPA 3B42RT retrievals based on AMSR-E/LSMEM  $\Delta$ SM is carried out using the methods described in Section 2.2.3, and results from the idealized experiment (Sect. 3) with regard to the circumstances where an adjustment is applied.

An example of TMPA 3B42RT adjustment is provide in Figure 8, where a snapshot of the rainfall field js shown (Figure 8b) and compared with NLDAS on May 26<sup>th</sup> 2006 and the adjusted rainfall pattern based on AMSR-E/LSMEM  $\Delta$ SM. The 3B42RT<sub>ADJ</sub> rainfall field (Figure 8c) is similar in terms of its spatial distribution compared to NLDAS precipitation estimates (Figure 8d).

On average TMPA 3B42RT and AMSR-E/LSMEM  $\Delta$ SM have a spatial Pearson Correlation Coefficient of 0.37 (Shown in Figure 9, left), compared to 0.52 for the correlation between NLDAS and  $\Delta$ SM. After the adjustment procedure, the Pearson correlation coefficient between 3B42RT<sub>ADJ</sub> and AMSR-E/LSMEM  $\Delta$ SM increases to 0.53, (shown in Figure 9), indicating that the correction method is successful. A below average increase in correlation is found over the western mountainous region, the Great Lakes region and eastern high vegetated and populated region. Additionally, the satellite soil moisture suffers from snow/ice/standing water contamination, which affects the potential for improved results after correction. The 3B42RT<sub>ADJ</sub> has significant improvement over 3B42RT in terms of long-term precipitation bias. The bias in 3B42RT annual mean precipitation is reduced by 20.6%, from -9.32mm/month spatial average in 3B42RT to -7.40mm/month in 3B42RT<sub>ADJ</sub> (shown in Figure 9, right). Frequency of rain days generally increases significantly everywhere, (Figure 10). The NLDAS data (Figure 10, right) suggests an almost constant drizzling rainfall over parts of the western mountainous area (Montana, Idaho, Wyoming and Colorado), while assimilating AMSR-E/LSMEM  $\Delta$ SM datasets does not have a signal of higher rainfall frequency, (Figure 10, middle). This is possibly due to lower soil moisture variability in satellite retrievals over the dry, mountainous areas and frequent presence of snow and ice (3B42RT is not updated under such circumstances).

Figure 11 shows the assimilation results for the grids and days with soil moisture observations, using the NLDAS precipitation as a reference. Overall, the method is

Authors 8/31/2015 3:38 PM

Deleted: Actual

Authors 8/31/2015 3:38 PM

Deleted: the

Authors 8/31/2015 3:38 PM

Deleted: Figure 8 shows

Authors 8/31/2015 3:38 PM

Deleted: from the 3B42RT

Authors 8/31/2015 3:38 PM

Deleted: product

Authors 8/31/2015 3:38 PM

Deleted: d).

Authors 8/31/2015 3:38 PM

Deleted: has

Authors 8/31/2015 3:38 PM

Deleted: average

Authors 8/31/2015 3:38 PM

Deleted: Figure.A1

Authors 8/31/2015 3:38 PM

Deleted: . There

Authors 8/31/2015 3:38 PM

Deleted: a smaller

Authors 8/31/2015 3:38 PM

Deleted: adjustment. In general, adjustment decreases rainfall amount while increases rain days (frequency of rainy days shown in Figure 9 and Figure 10).

Authors 8/31/2015 3:38 PM

Deleted: underestimated

Authors 8/31/2015 3:38 PM

Deleted: , which

Authors 8/31/2015 3:38 PM

Deleted: %

Authors 8/31/2015 3:38 PM

Deleted: Figure.A1

Authors 8/31/2015 3:38 PM

Deleted: .

Authors 8/31/2015 3:38 PM

Deleted: .

Authors 8/31/2015 3:38 PM

Deleted: ). The excessive 3B42RT<sub>ADJ</sub> rainfall events comes from the high-frequency noise in AMSR-E/LSMEM soil moisture retrievals identified by Pan et, al (2004) and Wanders et al. (2015)

Authors 8/31/2015 3:38 PM

Deleted: Figure 9 presents false alarm rate (FAR) and probability of detection (POD) of 3B42RT and 3B42RT<sub>ADJ</sub>, using NLDAS as reference dataset. The rain event threshold is set to be 0.1mm/day and 2mm/day. Cor... [1]

successful in correcting daily rainfall amount when 3B42RT overestimates precipitation,  $(3B42RT - NLDAS > 0)$ . Mean standard deviation (STD) of  $3B42RT_{ADJ} - NLDAS$  is between 1 and 3 mm/day (statistics provided in Table 3). When 3B42RT underestimates rainfall,  $(3B42RT - NLDAS < 0)$ , the assimilation has limited improvement on 3B42RT. This is due to the effect of surface saturation. In terms of adding rainfall, there are two scenarios when the effectiveness of the assimilation is limited.

- 1) The presence of wet conditions or (near) saturation. There is higher probability bringing the surface to saturation (wetter condition) when the assimilation adds rainfall into 3B42RT. However soil moisture increments are less sensitive to incoming precipitation on wetter soil. Therefore, an error in  $\Delta SM$  often translates into  $3B42RT_{ADJ}$  in a magnified manner.
- 2) The presence of very heavy precipitation, which typically brings the surface to saturation, hence not results in an update of 3B42RT, is not updated. If, by a small probability, the surface is wet (nearly saturated) but not completely saturated after a heavy rainfall, the updated 3B42RT also suffers from large uncertainty (explained in 1) above).

The effect of the assimilation conditioned on 3B42RT rainfall amount is further evaluated by skill scores. Figure 12 presents probability of detection (POD) and false alarm rate (FAR) in 3B42RT and  $3B42RT_{ADJ}$ , using NLDAS as the reference dataset. The rain event threshold is set to be 0.1 mm/day and 2 mm/day. This is possibly due to lower soil moisture variability in satellite retrievals over the dry, mountainous areas and frequent presence of snow and ice (3B42RT is not updated under such circumstances). For a 0.1 mm/day threshold, both FAR and POD increases in  $3B42RT_{ADJ}$  except for the mountainous region. Whereas for a 2 mm/day threshold, there is only slight increase in FAR in most of eastern U.S. region. The overestimation of rain days is also absent when 2 mm/day event threshold is applied which suggests that most of the excessive rainy days have less than 2 mm/day rain amount. Consistent with other studies, spatially, larger improvements are found in the central U.S. The area coincides where higher AMSR-E/LSMEM  $\Delta SM$  accuracy is found (non-mountainous regions with little urbanization and light vegetation). Despite of the regional variability, these excessive rainy days are a

Authors 8/31/2015 3:38 PM

Deleted: .

Authors 8/31/2015 3:38 PM

Deleted: 3mm

Authors 8/31/2015 3:38 PM

Deleted: ,

Authors 8/31/2015 3:38 PM

Deleted: a  $\Delta SM$

Authors 8/31/2015 3:38 PM

Deleted: to

Authors 8/31/2015 3:38 PM

Deleted: near

Authors 8/31/2015 3:38 PM

Deleted: a

Authors 8/31/2015 3:38 PM

Deleted: Since the prior knowledge of overestimated precipitation is not always available, the

Authors 8/31/2015 3:38 PM

Deleted: .



503 result of the high-frequency noise in AMSR-E/LSMEM soil moisture retrievals identified  
504 by Pan et al (2004) and Wanders et al. (2015).

505 The applied method is ineffective for light rainfall  $< 2$  mm, where the adjustment tends to  
506 over-correct precipitation by adding excessive rainfall – mostly the result of the high  
507 frequency AMSR-E noise. MAE of light rainfall ( $< 2$  mm/day) increased from 0.65  
508 mm/day in 3B42RT to 0.99 mm/day in 3B42RT<sub>ADJ</sub>. On the other hand, satellite soil  
509 moisture assimilation is very effective in correcting satellite precipitation larger than 2  
510 mm/day: MAE of medium to large rainfall ( $\geq 2$  mm/day) decreased from 7.07 mm/day in  
511 3B42RT to 6.55 mm/day in 3B42RT<sub>ADJ</sub>. The effect of the assimilation is different over  
512 the western mountainous region, the north-to-south central U.S. band and the eastern U.S.

513 The western mountainous region has a dry climatology with more frequent rainfall in  
514 small amounts. The white noise in  $\Delta$ SM, negatively impacting 3B42RT<sub>ADJ</sub>, is comparable  
515 to the positive improvement brought by actual light rainfall signals in  $\Delta$ SM. Therefore,  
516 the assimilation of  $\Delta$ SM has no significant impact in these regions.

517 The north-to-south band over central U.S. experiences more medium to large ( $\geq 2$   
518 mm/day) rainfall. In addition, the region is lightly vegetated (annual mean LAI  $< 1$ ) with  
519 low elevation ( $< 1500$  m), where soil moisture retrievals are of higher accuracy. Soil  
520 moisture climatology is wetter in the west, causing larger variations in 3B42RT<sub>ADJ</sub> error  
521 from the white noise  $\Delta$ SM (as discussed in Section 3.2). Despite of that, satellite soil  
522 moisture is most effective correcting medium to large rainfall under normal surface  
523 conditions.

524 The decreased skill in 3B42RT<sub>ADJ</sub> over eastern U.S. is primarily attributed to both  
525 precipitation and soil moisture climatology, a wet climate with more medium to large  
526 rainfall, neither of which is suitable for soil moisture assimilation.

527 In summary, the high-frequency noise in soil moisture product causes a major limitation.  
528 The noise impacts adjusted precipitation by introducing false alarm rain days. It is  
529 difficult to distinguish the noise and retrieve the true rainfall signals. A remedy to prevent  
530 the excessive rain days is applying a cutoff  $\Delta$ SM threshold when rain days are added, at  
531 the expense of neglecting a part of the true rainfall signals. Figure 13 shows the  
532 probability of added rainy days being consistent with NLDAS (NLDAS  $> 0$  mm/day)

Authors 8/31/2015 3:38 PM

Deleted: <2mm

Authors 8/31/2015 3:38 PM

Deleted: coming

Authors 8/31/2015 3:38 PM

Deleted: the high frequency AMSR-E noise.

Authors 8/31/2015 3:38 PM

Deleted: Satellite

Authors 8/31/2015 3:38 PM

Deleted: of larger than 2mm/day.

Authors 8/31/2015 3:38 PM

Deleted: amount. Skills are limited by the white noise in  $\Delta$ SM.

Authors 8/31/2015 3:38 PM

Deleted: real

Authors 8/31/2015 3:38 PM

Deleted: (

Authors 8/31/2015 3:38 PM

Deleted: -20mm

Authors 8/31/2015 3:38 PM

Deleted: 1500m

Authors 8/31/2015 3:38 PM

Deleted: than

Authors 8/31/2015 3:38 PM

Deleted: variation

Authors 8/31/2015 3:38 PM

Deleted: with

Authors 8/31/2015 3:38 PM

Deleted: condition

Authors 8/31/2015 3:38 PM

Deleted: is

Authors 8/31/2015 3:38 PM

Deleted: rainy

Authors 8/31/2015 3:38 PM

Deleted: of

Authors 8/31/2015 3:38 PM

Deleted: rainy

Authors 8/31/2015 3:38 PM

Deleted: rainy

Authors 8/31/2015 3:38 PM

Deleted: By comparing the distribution

with respect to  $\Delta SM$ . When a new rainy day is added ( $3B42RT = 0$  mm/day,  $3B42RT_{ADJ} > 0$  mm/day) based on AMSR-E/LSMEM  $\Delta SM$  of 2 mm/day, there's approximately 78% chance that the added rain day is a true event ( $NLDAS > 0$  mm/day); That is, approx. 22% chance that it is a false alarm ( $NLDAS = 0$  mm/day). When AMSR-E/LSMEM  $\Delta SM$  is larger than 2 mm/day, the probability of added rainy days being true event is even higher, up to 90% chance. Here we applied a threshold of 2 mm/day on AMSR-E/LSMEM  $\Delta SM$ . That is, when new rainy days are introduced ( $3B42RT > 0$ ,  $3B42RT_{ADJ} \geq 0$ ), we discard the update and keep the no-rain day if AMSR-E/LSMEM soil moisture increment is below 2 mm. Note that, the probability of the false alarms depends on soil moisture climatology: the wetter soil moisture climatology, the larger uncertainty in the signal. Therefore, this threshold should vary in accordance with local soil moisture climatology, i.e. a larger threshold over the wetter east U.S. and smaller threshold over the drier western U.S. Nevertheless, after the 2 mm/day  $\Delta SM$  threshold is applied, expectedly, the statistics are largely improved: FAR is decreased significantly from 0.519 (wo.  $\Delta SM$  threshold) to 0.066 (w.  $\Delta SM$  threshold). MAE of light rainfall ( $< 2$  mm/day) in  $3B42RT_{ADJ}$  decreased from 0.99 mm/day to 0.64 mm/day, compared to 0.65 mm/day in  $3B42RT$ . For medium to large  $3B42RT$  rainfall ( $\geq 2$  mm/day), it effectively increased POD (0.362 in  $3B42RT$  vs 0.386 in  $3B42RT_{ADJ}$  w.  $\Delta SM$  threshold) and decreased FAR (0.037 in  $3B42RT$  vs 0.030 in  $3B42RT_{ADJ}$  w.  $\Delta SM$  threshold). Further work is needed to characterize, distinguish and decrease the high-frequency noise in SM retrievals. Figure 13 gives an example of evaluating the impact of SM uncertainties in assimilation as curves derived over different topography can be quantitatively compared.

## 5 Comparison to other studies

Many other studies have utilized satellite microwave brightness temperatures or soil moisture retrievals to constrain satellite precipitation estimates (Pellarin et al., 2008), estimate precipitation (e.g. Brocca et al., 2013) or improve precipitation estimates through assimilation (Crow et al., 2009, 2011). Here, we review their approaches and findings in light of the results of this study, and compare our results with some of these studies to gain insight into their robustness and consistency.

Authors 8/31/2015 3:38 PM

**Deleted:**  $\Delta SM$

Authors 8/31/2015 3:38 PM

**Deleted:** falsely reported in  $3B42RT_{ADJ}$ , a cutoff  $\Delta SM$  threshold of 2mm/day could filter out 99.8% of the false alarms. The simple application of a spatially uniform, stationary cutoff  $\Delta SM$  threshold on the added rainy days could distinguish 3.3% of the true rain signals. The same evaluation metrics for

Authors 8/31/2015 3:38 PM

**Deleted:** after cutoff threshold is applied are provided in Figure 12c-d. Expectedly, the statistics are largely improved.

Authors 8/31/2015 3:38 PM

**Formatted:** Not Superscript/ Subscript

Authors 8/31/2015 3:38 PM

**Deleted:** rain amount

Authors 8/31/2015 3:38 PM

**Deleted:** Intensity-duration-frequency curves are also shown in Figure.A 2. Again, the difference in the performance of adjusted rainfall of selected grids is associated with local climatology. Thus

Authors 8/31/2015 3:38 PM

**Deleted:** However, it should also be noted that the application of the cutoff

Authors 8/31/2015 3:38 PM

**Deleted:** is not able to decrease uncertainties for

Authors 8/31/2015 3:38 PM

**Deleted:** .

Authors 8/31/2015 3:38 PM

**Deleted:** analyzed the assimilation of

Authors 8/31/2015 3:38 PM

**Deleted:** to

Authors 8/31/2015 3:38 PM

**Deleted:** . In the following

Authors 8/31/2015 3:38 PM

**Deleted:** qualitatively

Authors 8/31/2015 3:38 PM

**Deleted:** Our results confirm

Authors 8/31/2015 3:38 PM

**Moved up [1]:** the effect of surface saturation on adjusted precipitation, which is well described in previous studies (e.g. Brocca et al.,

Authors 8/31/2015 3:38 PM

**Deleted:** 2011, 2013).

Pellarin et al. (2008) used the temporal variations of the AMSR-E 6.7 GHz brightness temperature (TB) normalized polarization difference,  $PR=(TB_V-TB_H)/(TB_V+TB_H)$ , to screen out anomalous precipitation events from a 4-day cumulative satellite-estimated precipitation (EPSAT-SG: Chopin et al., 2005) from 22 to 26 of June 2004 over a 100 x 125 km box centered over Niger in west Africa. This was extended in Pellarin et al. (2013) where an API-based water balance model was used to correct three different satellite precipitation products (CMORPH, TRMM-3B42 and PERSIANN) over a 4-year period in west Africa at three 0.25° grids in Niger, Benin and Mali). The new algorithm was evaluated by comparing the corrected precipitation to estimates over the 0.25° grids from ground-based precipitation measurements. A sequential assimilation approach was applied where AMSR-E C-band TB measurements were used to estimate a simple multiplicative factor to the precipitation estimates in order to minimize the difference between observed (AMSR-E) and simulated TBs in term of root mean square error (RMSE). The results show improvements over those found in Pellarin et al. (2009). Specifically, the Pellarin et al. (2013) study shows that the proposed methodology produces an improvement of the RMSE at daily, decadal and monthly time scales and at the three locations. For instance, the RMS mean error decreases from 7.7 to 3.5 mm/day at the daily time scale in Niger and from 18.3 to 7.7 mm/day at the decadal time scale in Mali.

Crow et al. (2003, 2009, 2011) demonstrated the effectiveness of the assimilation of remotely sensed microwave brightness temperatures or retrieved soil moisture in estimating precipitation based on airborne measurements over the Southern Great Plains (USA) region (Crow et al., 2003); 2 to 10 day accumulated precipitation within a simple API water budget model and assimilation scheme over CONUS (Crow et al., 2009); and 3 day, 1° precipitation accumulation over three African Monsoon Multidisciplinary Analysis (AMMA) sites in west Africa with an enhanced assimilation scheme and an API-moisture model (Crow et al., 2011). Crow et al. (2009) recommends against estimating precipitation at a larger scale than three days based on assimilating AMSR-E/LSMEM soil moisture.

Brocca et al. (2013) estimated precipitation by inverting the water budget equation such that precipitation could be estimated from changes in soil moisture. The inverted equation

Authors 8/31/2015 3:38 PM

**Deleted:** In particular, Wanders et al. (2015, hereby W15) performed a comprehensive study using multiple satellite soil moisture (AMSR-E/LSMEM, ASCAT and SMOS) and land surface temperature data. This study focused exclusively on the usefulness of soil moisture product and differs in the pre-processing method (CDF-matching versus polynomial regression), the temporal period (2010-2011 versus 2002-2007) and the temporal resolution (3-hourly versus da... [2]

was calibrated using in-situ, 4-day averaged observations at two sites in Spain and Italy. In Brocca et al. (2014), the same approach was used globally for 5-day precipitation totals and at 1° spatially. Soil moisture observations from three satellite derived soil moisture datasets (AMSR-E LPRM, ASCAT and SMOS) were used. The soil moisture and rainfall were aggregated to a 1° spatial resolution, the soil moisture changes over a 5-day period to estimate a 5-day total precipitation. No formal data assimilation was carried out. The newly created precipitation data set was compared to two satellite precipitation products (TRMM-3B42RT, GPCC) and two gauge based precipitation products (GPCP, ERA-Interim). But they do note that their approach has “poor scores in reproducing daily rainfall data”. Nonetheless, these studies show promising results.

In the study reported here, three advances have been made over these earlier studies: (i) we adopted a state-of-the-art dynamic land surface model that has demonstrated high skill in simulating soil moisture when driven by high quality precipitation data (Schaafe et al., 2004); (ii) we applied a state-of-the-art data assimilation procedure based on particle filtering so as to extract (and hopefully maximize) the information content from the satellite most effectively; (iii) we increased the resolution of the precipitation estimation window down to 1 day, exceeding the conclusions in these earlier studies that the finest temporal resolution is 3 to 5 days. Additionally we increased (or matched) the spatial resolution to 0.25°, limited primarily by the satellite soil moisture product resolution; and (iv) previous studies are based on the assumption that the SM retrievals are 100% accurate and contain no errors. We evaluated this assumption by analyzing the impact of uncertainties associated with the soil moisture retrievals. These advances offer important benefits when satellite precipitation products are used for applications such as flood forecasting. Admittedly by aggregating in space and time, the improvement is more robust since some errors are averaged out. However improving satellite precipitation by AMSR-E/LSMEM SM is not entirely without skill. In fact, it could effectively correct rainfall with proper cautions given to local climatology where the assimilation is carried out.

Wanders et al. (2015) performed a comprehensive inter-comparison study using multiple satellite soil moisture and land surface temperature (LST) data at fine temporal scale (3-hourly). Compared to their study, ours focuses on using soil moisture exclusively from

one satellite and retrieval algorithm, and in improvements to the assimilation algorithm. Specifically in (i) the longer temporal period (2010-2011 in Wanders, et al. versus 2002-2007 in this study), (ii) the temporal resolution (3-hourly versus daily); (iii) the particle generation and bias correction method. We present in the paper improvements in the generation of rain particles and the bias-correction of the satellite soil moisture observations, as well as enhancements to the assimilation algorithm to maximize the information that can be gained from using soil moisture alone in adjusting precipitation. Due to the very strong and complicated spatial structure of precipitation, that is non-Gaussian and non-stationary in both time and space, a more advanced method is applied to generate possible precipitation fields than used or presented in earlier studies or in Wanders et al, (2015). Furthermore, a more advanced bias correction method is also applied to account for the reported problems (Wanders et al., 2015) in the second order statistics of the soil moisture retrievals; and (iv) SM retrieval products (and overpasses) used in assimilation. Our improved results are based on soil moisture retrievals from ascending overpasses only (versus both descending and ascending overpasses from multiple datasets, i.e. AMSR-E/LSMEM, ASCAT and SMOS). Our exclusive focus on the usefulness of soil moisture product promises more applicability especially for improving satellite precipitation from the Global Precipitation Mission products. The descending overpasses have generally better performance than the ascending, suggesting the potentials of further improvements.

A quantitative comparison of Wanders et al. (2015) and our results is provided below. Despite of the different time periods between Wanders et al. (2015, 2010-2011) and in our study (2002-2007), Wanders et al. (2015) shows decreasing POD (-15.0% to -46.4% depending on different products used) and FAR (-47.2% to -89.1% depending on different products used) for all rainfall after assimilation using either (single or multiple) SM products alone or SM + LST data combined (see Table 4 of Wanders et al., 2015). While in our study, after applying  $\Delta$ SM threshold, medium to large 3B42RT<sub>ADJ</sub> rainfall ( $\geq 2$  mm/day) has an increase in POD (+6.6%) and decrease in FAR (-18.9%). Furthermore, the significant dry bias in adjusted precipitation (see Fig.6 of Wanders et al., 2015) is not present in our results (Figure 9). This is due to improvements in our precipitation ensemble generation and bias correction scheme. Wanders et al. (2015)

Authors 8/31/2015 3:38 PM  
**Formatted:** Normal, No bullets or numbering

Authors 8/31/2015 3:38 PM  
**Deleted:** ; however, W15

Authors 8/31/2015 3:38 PM  
**Deleted:** and FAR

Authors 8/31/2015 3:38 PM  
**Deleted:** .

Authors 8/31/2015 3:38 PM  
**Deleted:** . W15

applied an additional step generating precipitation particles sampling from a 3×3 window, that over-eliminates most of the excessive rainfall, along with some real signal. We suggest loosening this constraint to a larger window size or to sample from adjusted precipitation instead of original 3B42RT precipitation. However sampling from adjusted precipitation at each time step, would significantly increase the computational demand, limiting the potential for a global application at high temporal/spatial resolution.

Furthermore, the outcome is quite different for the distribution of soil moisture retrievals after pre-processing (Fig.9 of Wanders et al. 2015 vs Figure 4 in our study) due to different methods used. After pre-processing, distributions of soil moisture retrievals is more similar to that of NLDAS precipitation forced, VIC modeled 1<sup>st</sup> layer soil moisture. CDF-matching used by Wanders et al., (2015) is based on the assumption that satellite soil moisture and modeled soil moisture respond to heavy rainfall in the same way, essentially having a rank correlation of 1. However that is not observed because of shallower detection depth of the satellite soil moisture. On the other hand, using the pre-processing method presented in this study, the signal of near-saturation in AMSR-E/LSMEM ΔSM tends to be overestimated after pre-processing, which indicates a heavy rain event that is often accompanied with surface saturation, and thus does not provide effective information for the assimilation. The other benefit of the 2<sup>nd</sup> order polynomial regression lies in its non-linearity. An error in the soil moisture product impacts the precipitation adjustment in a predictable way, allowing for a more systematic post-processing treatment. Based on the known error characteristics, we demonstrate a potential remedy to deal with the error by applying a 2 mm/day cutoff ΔSM threshold. Meanwhile, it is also highlighted that the cutoff threshold should be variable and positively correlated with local soil moisture climatology. We acknowledge that the soil moisture product used in Wanders et al. (2015), is a blended product of multiple satellite soil moisture datasets. It is not clear how its error characteristics impact the adjusted precipitation.

## 6 Conclusion and Discussion

Based on the retrieved soil moisture from AMSR-E using the LSMEM retrieval algorithm, we propose an assimilation procedure to integrate soil moisture information

Authors 8/31/2015 3:38 PM

Deleted: , which effectively filtered out

Authors 8/31/2015 3:38 PM

Deleted: . Note that applying such

Authors 8/31/2015 3:38 PM

Deleted: method, the independence of grid cells in VIC model is no longer maintained. This means that all grids need to be channeled after

Authors 8/31/2015 3:38 PM

Deleted: . Channeling grid cells

Authors 8/31/2015 3:38 PM

Deleted: computation efficiency

Authors 8/31/2015 3:38 PM

Deleted: when applying 0.1mm/day and 2mm/day event threshold (no significant increase in FAR for 2mm/day threshold); While in W15, decrease in both POD and FAR for 0mm/3hr and 2mm/3hr rain event threshold is reported. This is most likely due to the pre-processing method. CDF-matching

Authors 8/31/2015 3:38 PM

Deleted: .

Authors 8/31/2015 3:38 PM

Deleted: true

Authors 8/31/2015 3:38 PM

Deleted: ,

Authors 8/31/2015 3:38 PM

Deleted: in

Authors 8/31/2015 3:38 PM

Deleted: Error

Authors 8/31/2015 3:38 PM

Deleted: proper

Authors 8/31/2015 3:38 PM

Deleted: demonstrated

Authors 8/31/2015 3:38 PM

Deleted: 2mm

Authors 8/31/2015 3:38 PM

Deleted: W15

Authors 8/31/2015 3:38 PM

Deleted: model



779 into the VIC land surface model so as to improve real-time, satellite precipitation  
780 estimates. The ability to estimate rainfall amount is now enhanced with the above  
781 improvements, especially for [correcting](#) medium rainfall amounts. However, constrained  
782 by the noise in [AMSRE-TBs](#) and [thus](#) soil moisture retrievals, the assimilation is not  
783 effective in detecting missed rainfall events. The improved precipitation estimates,  
784 referred to as 3B42RT<sub>ADJ</sub> estimates, are overall consistent in reproducing the spatial  
785 pattern and time series of daily rainfall from NLDAS precipitation. The results illustrate  
786 the potential benefits of using data assimilation to merge satellite retrievals of surface soil  
787 moisture into a land surface model forced with real-time precipitation. Potentially the  
788 method can be applied globally for areas meeting vegetation cover and surface condition  
789 constraints that allows for soil moisture retrievals. Under these conditions, the approach  
790 can provide a supplementary source of information for enhancing the quality of satellite  
791 rainfall estimation, especially over poorly gauged areas like Africa.

Authors 8/31/2015 3:38 PM  
Deleted: correction

792 Nonetheless, some caution is required. The results of this study [show](#) that the adjusted  
793 real-time precipitation tends to add additional rain (frequency) resulting in more time  
794 steps with rain but lower regional average in the [western U.S.](#) and slightly higher regional  
795 average in [the](#) eastern U.S. It is also noticed that the precipitation adjustments are  
796 insensitive [under](#) saturated soil moisture conditions. A wetter surface magnifies any error  
797 associated with satellite observation by incorrectly adjusting precipitation. These errors,  
798 mixed with the “real” signal, generally add approximately ~2mm of precipitation (or  
799 higher) depending on the soil moisture climatology. It is important to consider these  
800 circumstances when observations are used so as to avoid introducing additional error.  
801 With these identified limitations, continued research is needed to assess the biases in the  
802 real-time precipitation retrievals on a local to regional basis so the assimilation system  
803 can be modified accordingly.

Authors 8/31/2015 3:38 PM  
Deleted: shows

Authors 8/31/2015 3:38 PM  
Deleted: West

Authors 8/31/2015 3:38 PM  
Deleted: with

804 The assimilation scheme used here assumed that the errors were attributed to the real-  
805 time precipitation retrievals, but the precipitation estimates after adjustment includes  
806 errors from additional sources. The two primary sources are errors in soil moisture  
807 retrievals and errors in the land surface model that include model parameterizations  
808 (poorly or insufficiently represented processes as well as scale issues) and parameter  
809 errors (insufficient calibration). There are also errors in other model forcing fields besides

814 precipitation. Further studies are needed to assess the attribution of these error sources to  
815 the total error. Such research will further improve the use of real-time satellite-based  
816 precipitation for global flood monitoring.

817 Besides the clear, heavy dependency of the assimilation effectiveness on the accuracy of  
818 satellite soil moisture product, it is also important to acquire adequate knowledge on the  
819 error characteristics of satellite soil moisture retrievals. Knowledge of the soil moisture  
820 errors could be important and the assimilation methods (including precipitation ensemble  
821 generation and pre-/post-processing method) should be chosen accordingly. On the other  
822 hand, the presence of data gaps between overpasses could be a large source of uncertainty  
823 with data assimilation. Further effort towards reliable spatial-temporal continuous (gap  
824 filled) satellite soil moisture datasets is needed.

825 While it has been illustrated in this study that the enhancement of real time satellite  
826 precipitation estimates can be realized through an assimilation approach using satellite  
827 soil moisture data products and a particle filter, additional satellite-based observations  
828 (e.g. multi-sensor soil moisture products) or variables (e.g. land surface temperatures as  
829 shown in Wanders et al. 2015, inundated areas), could be added/replaced in the  
830 assimilation process with different levels of complexity; e.g. by applying constraints on  
831 the particle generation. This opens up a great number of opportunities in using space-  
832 borne observations for supplementing direct retrievals of precipitation.

### 833 Acknowledgements

834 This research was supported through NASA grant NNX13AG97G (Multi-sensor  
835 enhancement of real-time satellite precipitation retrievals for improved drought  
836 monitoring) under the Precipitation Measurement Mission. Part of this research was  
837 financially supported by NWO Rubicon 825.15.003. This support is gratefully  
838 acknowledged.

839

Authors 8/31/2015 3:38 PM

Deleted: on

Authors 8/31/2015 3:38 PM

Deleted: error

Authors 8/31/2015 3:38 PM

Deleted: in

Authors 8/31/2015 3:38 PM

Deleted: area

Authors 8/31/2015 3:38 PM

Deleted: apply constrains

Authors 8/31/2015 3:38 PM

Formatted: English (UK)

Authors 8/31/2015 3:38 PM

Deleted: Page Break



## References

- Brocca, L., Melone, F., Moramarco, T. and Morbidelli, R.: Antecedent wetness conditions based on ERS scatterometer data, *J. Hydrol.*, 364(1-2), 73–87, doi:10.1016/j.jhydrol.2008.10.007, 2009.
- Brocca, L., Moramarco, T., Melone, F. and Wagner, W.: A new method for rainfall estimation through soil moisture observations, *Geophys. Res. Lett.*, 40(5), 853–858, doi:10.1002/grl.50173, 2013.
- Brocca, L., Ciabatta, L., Massari, C., Moramarco, T., Hahn, S., Hasenauer, S., Kidd, R., Dorigo, W., Wagner, W. and Levizzani, V.: Soil as a natural rain gauge: Estimating global rainfall from satellite soil moisture data, *J. Geophys. Res. Atmos.*, 119(9), 5128–5141, doi:10.1002/2014JD021489, 2014.
- [Chopin, F., Berges, J., Desbois, M., Jobard, I. and Lebel, T.: Satellite Rainfall Probability and Estimation. Application to the West Africa During the 2004 Rainy Season, AGU Spring Meet. Abstr., A12, 2005.](#)
- Crow, W. T.: Correcting land surface model predictions for the impact of temporally sparse rainfall rate measurements using an ensemble Kalman filter and surface brightness temperature observations, *J. Hydrometeorol.*, 4(5), 960–973, 2003.
- Crow, W. T., Huffman, G. J., Bindlish, R. and Jackson, T. J.: Improving Satellite-Based Rainfall Accumulation Estimates Using Spaceborne Surface Soil Moisture Retrievals, *J. Hydrometeorol.*, 10(1), 199–212, doi:10.1175/2008JHM986.1, 2009.
- Crow, W. T., Van Den Berg, M. J., Huffman, G. J. and Pellarin, T.: Correcting rainfall using satellite-based surface soil moisture retrievals: The Soil Moisture Analysis Rainfall Tool (SMART), *Water Resour. Res.*, 47(8), 1–15, doi:10.1029/2011WR010576, 2011.
- [Dee, D. P., Uppala, S. M., Simmons, A. J., Berrisford, P., Poli, P., Kobayashi, S., Andrae, U., Balmaseda, M. A., Balsamo, G., Bauer, P. and others: The ERA-Interim reanalysis: Configuration and performance of the data assimilation system, \*Q. J. R. Meteorol. Soc.\*, 137\(656\), 553–597, 2011.](#)

874 Ebert, E. E., Janowiak, J. E. and Kidd, C.: Comparison of near-real-time precipitation  
875 estimates from satellite observations and numerical models, *Bull. Am. Meteorol. Soc.*,  
876 88(1), 47–64, doi:10.1175/BAMS-88-1-47, 2007.

877 Ek, M. B., Xia, Y., Wood, E., Sheffield, J., Luo, L., Lettenmaier, D., Livneh, B., Mocko,  
878 D., Cosgrove, B., Meng, J., Wei, H., Koren, V., Schaake, J., Mo, K., Fan, Y. and Duan,  
879 Q.: North American Land Data Assimilation System Phase 2 (NLDAS-2): Development  
880 and Applications, *GEWEX Newsl.*, 21(2), 5–7, 2011.

881 Francois, C., Quesney, A. and Ottlé, C.: SAR Data into a Coupled Land Surface–  
882 Hydrological Model Using an Extended Kalman Filter, *J. Hydrometeorol.*, 4(2), 473–487,  
883 doi:10.1175/1525-7541(2003)4<473:SAOESD>2.0.CO;2, 2003.

884 Gao, H., Tang, Q., Shi, X., Zhu, C., Bohn, T. J., Su, F., She eld, J., Pan, M., and Wood,  
885 E. F.: Water budget record from Variable Infiltration Capacity (VIC) model, in:  
886 Algorithm Theoretical Basis Document for Terrestrial Water Cycle Data Records (in  
887 review), 2010.

888 Huffman, G. J., Bolvin, D. T., Nelkin, E. J., Wolff, D. B., Adler, R. F., Gu, G., Hong, Y.,  
889 Bowman, K. P. and Stocker, E. F.: The TRMM Multisatellite Precipitation Analysis  
890 (TMPA): Quasi-Global, Multiyear, Combined-Sensor Precipitation Estimates at Fine  
891 Scales, *J. Hydrometeorol.*, 8(1), 38–55, doi:10.1175/JHM560.1, 2007.

892 Huffman, G. J., Adler, R. F., Bolvin, D. T., and Nelkin, E. J.: The TRMM Multi-satellite  
893 Precipitation Analysis (TMPA), in: *Satellite Rainfall Applications for Surface*  
894 *Hydrology*, Springer Netherlands, 3–22, 2010.

895 Kalman, R. E.: A New Approach to Linear Filtering and Prediction Problems, *J. Basic*  
896 *Eng.*, 82(1), 35, doi:10.1115/1.3662552, 1960.

897 [Kerr, Y. H., Waldteufel, P., Richaume, P., Wigneron, J.-P., Ferrazzoli, P., Mahmoodi, A.,](#)  
898 [Al Bitar, A., Cabot, F., Gruhier, C., Juglea, S. E., Leroux, D., Mialon, A. and Delwart, S.:](#)  
899 [The SMOS Soil Moisture Retrieval Algorithm, \*Geosci. Remote Sensing, IEEE Trans.\*,](#)  
900 [50\(5\), 1384–1403, doi:10.1109/TGRS.2012.2184548, 2012.](#)

901 Liang, X., Lettenmaier, D. P., Wood, E. F. and Burges, S. J.: A simple hydrologically  
 902 based model of land surface water and energy fluxes for general circulation models, *J.*  
 903 *Geophys. Res.*, 99, 14415–14428, doi:10.1029/94JD00483, 1994.

904 Liang, X., Wood, E. F. and Lettenmaier, D. P.: Surface soil moisture parameterization of  
 905 the VIC-2L model: Evaluation and modification, *Glob. Planet. Change*, 13(1-4), 195–  
 906 206, doi:10.1016/0921-8181(95)00046-1, 1996.

907 Massari, C., Brocca, L., Moramarco, T., Tramblay, Y. and Didon Lescot, J.-F.: Potential  
 908 of soil moisture observations in flood modelling: estimating initial conditions and  
 909 correcting rainfall, *Adv. Water Resour.*, 74, 44–53, doi:10.1016/j.advwatres.2014.08.004,  
 910 2014.

911 Matgen, P., Fenicia, F., Heitz, S., Plaza, D., de Keyser, R., Pauwels, V. R. N., Wagner,  
 912 W. and Savenije, H.: Can ASCAT-derived soil wetness indices reduce predictive  
 913 uncertainty in well-gauged areas? A comparison with in situ observed soil moisture in an  
 914 assimilation application, *Adv. Water Resour.*, 44, 49–65,  
 915 doi:10.1016/j.advwatres.2012.03.022, 2012.

916 McCabe, M. F., Wood, E. F. and Gao, H.: Initial soil moisture retrievals from AMSR-E:  
 917 Multiscale comparison using in situ data and rainfall patterns overs Iowa, *Geophys. Res.*  
 918 *Lett.*, 32(6), 1–4, doi:10.1029/2004GL021222, 2005.

919 Pan, M. and Wood, E. F.: Data Assimilation for Estimating the Terrestrial Water Budget  
 920 Using a Constrained Ensemble Kalman Filter, *J. Hydrometeorol.*, 7(3), 534–547,  
 921 doi:10.1175/JHM495.1, 2006.

922 Pan, M., Li, H. and Wood, E.: Assessing the skill of satellite-based precipitation  
 923 estimates in hydrologic applications, *Water Resour. Res.*, 46(9), W09535,  
 924 doi:10.1029/2009WR008290, 2010.

925 Pan, M., Sahoo, A. K. and Wood, E. F.: Improving soil moisture retrievals from a  
 926 physically-based radiative transfer model, *Remote Sens. Environ.*, 140, 130–140,  
 927 doi:10.1016/j.rse.2013.08.020, 2014.

928 Pellarin, T., Ali, A., Chopin, F., Jobard, I. and Bergès, J. C.: Using spaceborne surface  
 929 soil moisture to constrain satellite precipitation estimates over West Africa, *Geophys.*  
 930 *Res. Lett.*, 35(2), 3–7, doi:10.1029/2007GL032243, 2008.

931 Pellarin, T., Louvet, S., Gruhier, C., Quantin, G. and Legout, C.: A simple and effective  
 932 method for correcting soil moisture and precipitation estimates using AMSR-E  
 933 measurements, *Remote Sens. Environ.*, 136, 28–36, doi:10.1016/j.rse.2013.04.011, 2013.

934 Robock, A., Luo, L., Wood, E. F., Wen, F., Mitchell, K., Houser, P., Schaake, J.,  
 935 Lohmann, D., Cosgrove, B., Sheffield, J., Duan, Q., Higgins, W., Pinker, R., Tarpley, D.,  
 936 Basara, J. and Crawford, K.: Evaluation of the North American Land Data Assimilation  
 937 System over the southern Great Plains during the warm season, *J. Geophys. Res.*,  
 938 108(D22), 8846, doi:10.1029/2002JD003245, 2003.

939 Schaake, J. C., Duan, Q., Koren, V., Mitchell, K. E., Houser, P. R., Wood, E. F., Robock,  
 940 A., Lettenmaier, D. P., Lohmann, D., Cosgrove, B., Sheffield, J., Luo, L., Higgins, R. W.,  
 941 Pinker, R. T., and Tarpley, J. D.: An intercomparison of soil moisture fields in the North  
 942 American Land Data Assimilation System (NLDAS), *J. Geophys. Res. Atmos.*, 109(D1),  
 943 doi:10.1029/2002JD003309, 2004.

944 Schamm, K., M. Ziese, A. Becker, P. Finger, A. Meyer-Christoffer, U. Schneider, M.  
 945 Schröder, and P. Stender (2014), Global gridded precipitation over land: A description of  
 946 the new GPCC First Guess Daily product, *Earth Syst. Sci. Data*, 6, 49–60

947 Sorooshian, S.: Commentary-GEWEX (Global Energy and Water Cycle Experiment) at  
 948 the 2004 Joint Scientific Committee Meeting, *GEWEX Newsl.*, 14(2), 2, 2004.

949 Wanders, N., Pan, M. and Wood, E. F.: Correction of real-time satellite precipitation with  
 950 multi-sensor satellite observations of land surface variables, *Remote Sens. Environ.*, 160,  
 951 206–221, doi:10.1016/j.rse.2015.01.016, 2015.

952 Wu, H., Adler, R. F., Tian, Y., Huffman, G. J., Li, H. and Wang, J.: Real-time global  
 953 flood estimation using satellite-based precipitation and a coupled land surface and routing  
 954 model. *Water Resour. Res.*, 50(3), 2693–2717, doi:10.1002/2013WR014710, 2014.

Authors 8/31/2015 3:38 PM  
Deleted: . Y

Authors 8/31/2015 3:38 PM  
Moved (insertion) [2]

Authors 8/31/2015 3:38 PM  
Moved (insertion) [3]

Authors 8/31/2015 3:38 PM  
Moved (insertion) [4]

Authors 8/31/2015 3:38 PM  
Moved (insertion) [5]

Authors 8/31/2015 3:38 PM  
Moved up [2]: Robock, A., Lettenmaier, D. P., Lohmann, D., Cosgrove, B.,

Authors 8/31/2015 3:38 PM  
Moved up [3]: Higgins, R. W., Pinker, R. T

Authors 8/31/2015 3:38 PM  
Deleted: .,

Authors 8/31/2015 3:38 PM  
Moved up [4]: and Tarpley, J. D.: An intercomparison of soil moisture fields in the North American Land Data

Authors 8/31/2015 3:38 PM  
Moved up [5]: Geophys.

Authors 8/31/2015 3:38 PM  
Deleted: She eld, J., Luo, L. F.,

Authors 8/31/2015 3:38 PM  
Deleted: Assimilation System (NLDAS), J.

Authors 8/31/2015 3:38 PM  
Deleted: Res., 109(D1), D01S90, doi:10.1029/2002JD003309, 2004. .

Authors 8/31/2015 3:38 PM  
Deleted: —————Page Break—————

971 [List of Tables](#)

972 [Tables](#)

973 Table 1 Error statistics of recovered precipitation and effect of surface saturation in the idealized experiment (mm/day).

974 Table 2 Error statistics of recovered NLDAS based on  $\Delta SM$  (with added errors) conditioned on 1<sup>st</sup> layer soil wetness for the idealized  
975 experiment (mm/day).

976 Table 3 Error statistics of 3B42RT and 3B42RT<sub>ADJ</sub> compared to NLDAS precipitation (mm/day)

Authors 8/31/2015 3:38 PM

Deleted:

Unknown

Formatted: Font:(Default) Helvetica, 6 pt

## List of Figures

Figure 1 Schematic for [the](#) dynamic assimilation of AMSR-E/LSMEM  $\Delta$ SM into TMPA (3B42RT) [with the particle filter \(PF\)](#).

Figure 2 Schematic for [the strategy for processing](#) prior and posterior probability [densities](#) in [the](#) particle filter.

Figure 3 Statistics of NLDAS precipitation given 3B42RT precipitation measurement.

Boxplot shows the minimum, 15% quantile, 30% quantile, median, 70% quantile, 85% quantile and maximum value of NLDAS precipitation given 3B42RT precipitation in a certain bin.

Figure 4 Empirical cumulative distribution function of changes in soil moisture from top layer soil moisture from NLDAS precipitation forced VIC simulation (black), and AMSR-E/LSMEM soil moisture retrieval before (red) and after (blue) pre-processing.

Figure 5 Two cases with recovered spatial rainfall pattern in [the](#) idealized experiment after merging satellite soil moisture retrieval on: (a-e) 27<sup>th</sup> Oct. 2003 and (f-j) 22<sup>th</sup> Mar. 2006.

[Figure 6 Accuracy of recovered precipitation in idealized experiment: \(a\) overall performance and separately comparing the improvement performance of recovered NLDAS precipitation \(b\) with and \(c\) without surface saturation condition. Statistics provided in Table 1.](#)

Figure 7 Error in recovered NLDAS precipitation given surface moisture condition.

Recovered NLDAS is based on using “truth” soil moisture and soil moisture with normal error:  $N(0, \text{1mm})$ ,  $N(0, \text{2mm})$ ,  $N(0, \text{3mm})$ ,  $N(0, \text{4mm})$  and  $N(0, \text{5mm})$ . Statistics provided in Table 2.

1001 | Figure 8 May 26<sup>th</sup> 2006 Rainfall pattern in 3B42RT (b) against NLDAS (d) as detected  
1002 | by AMSR-E/LSMEM  $\Delta$ SM (a), and recovered rainfall field ( $3B42RT_{ADJ}$ ) by assimilating  
1003 | AMSR-E/LSMEM  $\Delta$ SM (c). Gray shading shows area without soil moisture retrievals.  
1004 | Figure 9 [Pearson correlation coefficient between AMSR-E/LSMEM  \$\Delta\$ SM and](#)  
1005 | [precipitation: a\) NLDAS, b\) 3B42RT and c\) 3B42RT<sub>ADJ</sub>; annual mean precipitation in d\)](#)  
1006 | [NLDAS, e\) 3B42RT and f\) 3B42RT<sub>ADJ</sub> of time steps with AMSR-E/LSMEM  \$\Delta\$ SM](#)  
1007 | [retrievals.](#)  
1008 | [Figure 10 Frequency of rainy days in 3B42RT, 3B42RT<sub>ADJ</sub> and NLDAS with a\) 0.1](#)  
1009 | [mm/day and b\) 2 mm/day rainfall threshold to define a rain day.](#)  
1010 | Figure 11 Distribution of 3B42RT and 3B42RT<sub>ADJ</sub> precipitation error compared to  
1011 | NLDAS. Statistics are provided in Table 3.  
1012 | Figure 12 [FAR and POD of 3B42RT and 3B42RT<sub>ADJ</sub> with a\) 0.1 mm/day and b\) 2](#)  
1013 | [mm/day rainfall threshold to define a rain event.](#)  
1014 | Figure 13 [Probability that the added rainy days \( \$3B42RT = 0\$  mm/day,  \$3B42RT\_{ADJ} > 0\$](#)   
1015 | [mm/day\) are true rain events \( \$NLDAS > 0\$  mm/day\) given corresponding AMSR-](#)  
1016 | [E/LSMEM  \$\Delta\$ SM.](#)  
1017 |

## Tables

Table 1 Error statistics of recovered precipitation and effect of surface saturation in the idealized experiment (mm/day).

		[3B42RT]-	0	0~0.2	0.2~0.5	0.5~1.0	1.0~1.5	1.5~2	2~2.5	2.5~5.0	5.0~7.5	7.5~10	10~15	15~20	20~25	>25
		[Recovered NLDAS]-[NLDAS]														
All surface	Bias		0.24	0.20	0.37	0.51	0.71	0.87	1.09	0.67	1.16	1.30	2.51	3.32	3.75	3.95
conditions	MAE		0.40	0.42	0.66	0.86	1.14	1.41	1.70	1.48	2.24	2.63	4.21	5.56	6.70	9.76
Unsaturated	Bias		0.23	0.19	0.29	0.40	0.52	0.68	0.82	0.65	1.10	1.27	2.19	2.88	3.14	3.14
surface	MAE		0.39	0.41	0.59	0.75	0.95	1.21	1.43	1.45	2.17	2.58	3.88	5.11	6.07	8.94
Saturated	Bias		2.31	5.06	47.65	42.58	50.67	44.09	59.64	6.83	16.09	9.19	46.47	57.98	65.33	64.09
surface	MAE		3.35	5.54	48.71	43.73	52.43	46.96	61.85	9.64	21.42	15.01	49.07	60.78	69.53	70.73

Deleted: <sp>

Unknown

Formatted

... [3]

Authors 8/31/2015 3:38 PM

Formatted Table

... [4]

Authors 8/31/2015 3:38 PM

Formatted

... [5]

Authors 8/31/2015 3:38 PM

Formatted

... [6]

Authors 8/31/2015 3:38 PM

Formatted

... [7]

Authors 8/31/2015 3:38 PM

Formatted

... [15]

Authors 8/31/2015 3:38 PM

Formatted

... [8]

Authors 8/31/2015 3:38 PM

Formatted

... [9]

Authors 8/31/2015 3:38 PM

Formatted

... [10]

Authors 8/31/2015 3:38 PM

Formatted

... [11]

Authors 8/31/2015 3:38 PM

Formatted

... [12]

Authors 8/31/2015 3:38 PM

Formatted

... [13]

Authors 8/31/2015 3:38 PM

Formatted

... [14]

Authors 8/31/2015 3:38 PM

Formatted

... [16]

Authors 8/31/2015 3:38 PM

Formatted

... [17]

Authors 8/31/2015 3:38 PM

Formatted

... [18]

Authors 8/31/2015 3:38 PM

Formatted

... [19]

Authors 8/31/2015 3:38 PM

Deleted: 092

Authors 8/31/2015 3:38 PM

Deleted: 155

Authors 8/31/2015 3:38 PM

Formatted

... [20]

Authors 8/31/2015 3:38 PM

Deleted: 238

Authors 8/31/2015 3:38 PM

Formatted

... [21]

Authors 8/31/2015 3:38 PM

Formatted

... [22]

Authors 8/31/2015 3:38 PM

Formatted

... [23]

Authors 8/31/2015 3:38 PM

Formatted

Authors 8/31/2015 3:38 PM

Formatted

Authors 8/31/2015 3:38 PM

Formatted



Table 2 Error statistics of recovered NLDAS based on  $\Delta SM$  (with added errors) conditioned on 1<sup>st</sup> layer soil wetness for the idealized experiment (mm/day).

[VIC 1st layer SM] - [maximum]* [Recovered NLDAS]-[NLDAS] [mm/day]		<-30	-30~-25	-25~-20	-20~-15	-15~-12	-12~-10	-10~-9	-9~-8	>-8
No error	Median	0.04	0.03	0.02	0.02	0.02	0.03	0.03	0.04	0.16
	IQR	0.14	0.08	0.07	0.07	0.08	0.12	0.21	0.29	1.71
1.0	Median	0.86	1.07	1.08	1.03	0.99	0.97	0.97	0.94	0.66
	IQR	1.52	1.72	1.77	1.83	1.96	2.08	2.14	2.19	2.59
2.0	Median	0.68	1.07	1.40	1.56	1.52	1.44	1.51	1.64	1.54
	IQR	1.76	2.09	2.88	3.45	3.63	3.73	3.73	3.73	3.91
3.0	Median	0.15	0.80	1.20	1.41	1.47	1.51	1.65	1.84	1.88
	IQR	1.36	2.16	3.04	3.73	3.74	3.79	4.34	5.24	5.47
4.0	Median	0.22	0.56	0.83	1.15	1.30	1.40	1.63	1.88	1.97
	IQR	0.99	2.36	2.48	3.99	4.05	4.70	5.53	5.52	5.63
5.0	Median	0.00	0.15	0.52	0.90	1.10	1.27	1.54	1.81	1.89
	IQR	1.62	2.54	2.91	4.43	4.51	5.95	5.90	5.79	7.04

\*1<sup>st</sup> layer soil depth is 100mm with a SM capacity of ~45mm depending on porosity.

Formatted ... [113]

Authors 8/31/2015 3:38 PM

Deleted: <sp> ... [114]

Unknown

Formatted ... [115]

Authors 8/31/2015 3:38 PM

Formatted Table ... [116]

Unknown

Formatted ... [117]

Authors 8/31/2015 3:38 PM

Formatted ... [118]

Authors 8/31/2015 3:38 PM

Formatted ... [119]

Authors 8/31/2015 3:38 PM

Formatted ... [120]

Authors 8/31/2015 3:38 PM

Formatted ... [121]

Authors 8/31/2015 3:38 PM

Formatted ... [122]

Authors 8/31/2015 3:38 PM

Formatted ... [123]

Authors 8/31/2015 3:38 PM

Formatted ... [124]

Authors 8/31/2015 3:38 PM

Formatted ... [125]

Authors 8/31/2015 3:38 PM

Formatted ... [126]

Authors 8/31/2015 3:38 PM

Deleted: 035

Authors 8/31/2015 3:38 PM

Deleted: 041

Authors 8/31/2015 3:38 PM

Formatted ... [137]

Authors 8/31/2015 3:38 PM

Deleted: 159

Authors 8/31/2015 3:38 PM

Formatted ... [130]

Authors 8/31/2015 3:38 PM

Deleted: 027

Authors 8/31/2015 3:38 PM

Deleted: 023

Authors 8/31/2015 3:38 PM

Formatted ... [131]

Authors 8/31/2015 3:38 PM

Deleted: 019

Authors 8/31/2015 3:38 PM

Authors 8/31/2015 3:38 PM

Formatted ... [133]

Authors 8/31/2015 3:38 PM

Authors 8/31/2015 3:38 PM

Formatted ... [127]

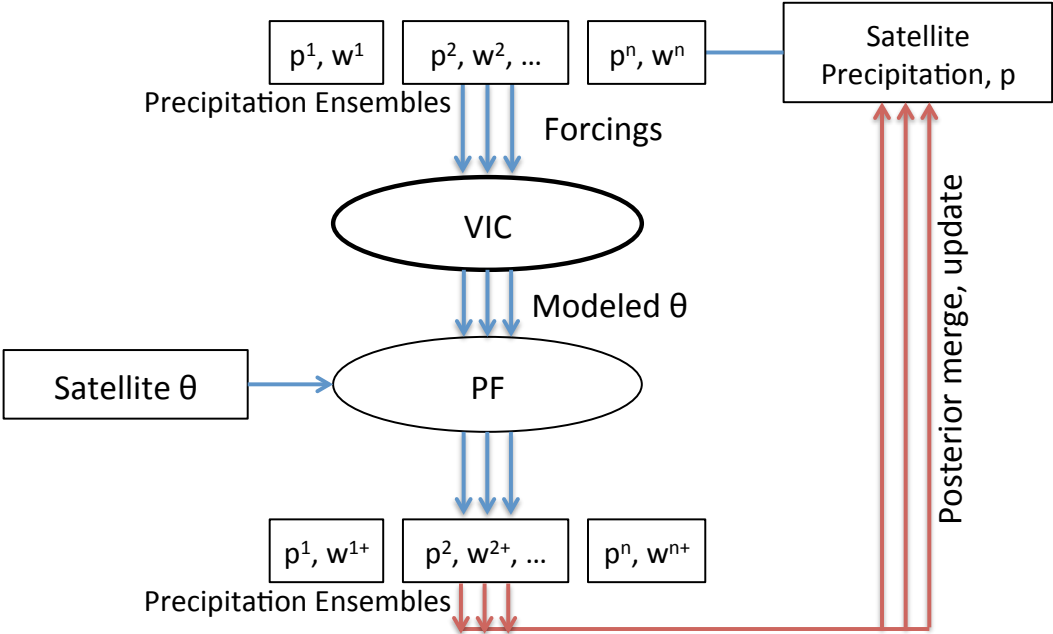
Authors 8/31/2015 3:38 PM

Formatted

Table 3 Error statistics of 3B42RT and 3B42RT<sub>ADJ</sub> compared to NLDAS precipitation (mm/day)

[3B42RT] - [NLDAS] [mm/day]		<-25	-25~-20	-20~-15	-15~-10	-10~-5	-5~-2	-2~-0.5	-0.5~0	0.5~2	2~5	5~10	10~15	15~20	20~25	>25
[3B42RT]																
Mean		-32.32	-22.19	-17.13	-12.09	-6.98	-3.22	-1.09	-0.02	1.11	3.20	6.87	11.96	16.97	21.95	27.35
STD		8.52	1.42	1.42	1.42	1.39	0.85	0.43	0.12	0.43	0.84	1.37	1.39	1.37	1.38	2.08
[3B42RT <sub>ADJ</sub> ]																
Mean		-31.24	-20.31	-14.79	-9.69	-4.81	-1.60	0.16	1.08	0.44	0.21	0.02	-0.06	0.00	-0.03	-0.12
STD		11.03	6.40	6.12	5.34	4.08	2.73	1.88	1.18	1.86	2.29	2.60	2.91	3.01	2.74	2.41

Formatted	... [245]
Authors 8/31/2015 3:38 PM	
Formatted	... [249]
Authors 8/31/2015 3:38 PM	
Formatted	... [251]
Authors 8/31/2015 3:38 PM	
Formatted	... [252]
Authors 8/31/2015 3:38 PM	
Formatted	... [253]
Authors 8/31/2015 3:38 PM	
Formatted	... [255]
Authors 8/31/2015 3:38 PM	
Formatted	... [260]
Authors 8/31/2015 3:38 PM	
Formatted	... [256]
Authors 8/31/2015 3:38 PM	
Formatted	... [258]
Authors 8/31/2015 3:38 PM	
Formatted	... [259]
Authors 8/31/2015 3:38 PM	
Formatted	... [262]
Authors 8/31/2015 3:38 PM	
Formatted	... [263]
Authors 8/31/2015 3:38 PM	
Formatted	... [246]
Authors 8/31/2015 3:38 PM	
Formatted	... [250]
Authors 8/31/2015 3:38 PM	
Formatted Table	... [247]
Authors 8/31/2015 3:38 PM	
Formatted	... [261]
Authors 8/31/2015 3:38 PM	
Formatted	... [264]
Authors 8/31/2015 3:38 PM	
Formatted	... [265]
Authors 8/31/2015 3:38 PM	
Formatted	... [266]
Authors 8/31/2015 3:38 PM	
Formatted	... [267]
Authors 8/31/2015 3:38 PM	
Formatted	... [268]
Authors 8/31/2015 3:38 PM	
Formatted	... [269]
Authors 8/31/2015 3:38 PM	
Formatted	... [248]
Authors 8/31/2015 3:38 PM	
Formatted	... [254]
Authors 8/31/2015 3:38 PM	
Formatted	... [257]
Authors 8/31/2015 3:38 PM	
Formatted	... [274]
Authors 8/31/2015 3:38 PM	



1545

1546 Figure 1 Schematic for the dynamic assimilation of AMSR-E/LSMEM  $\Delta$ SM into TMPA (3B42RT) with the particle filter (PF).

1547

Authors 8/31/2015 3:38 PM

$p^1, w^1$

Precipitation Er

(

Satellite  $\theta$

)

$p^1, w^{1+}$

Precipitation Er

Deleted:

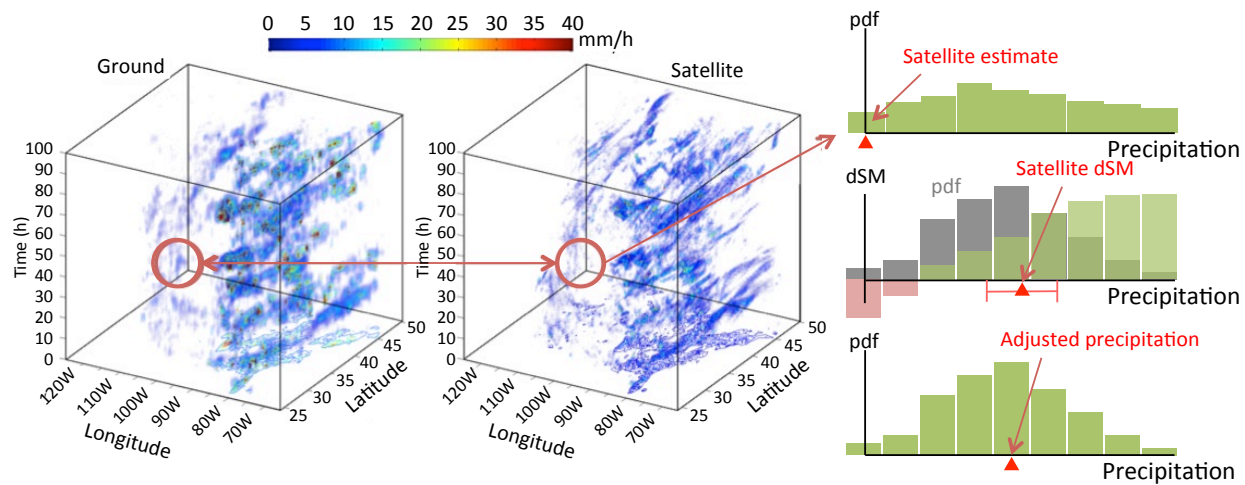
Authors 8/31/2015 3:38 PM

Deleted: of particle filtering

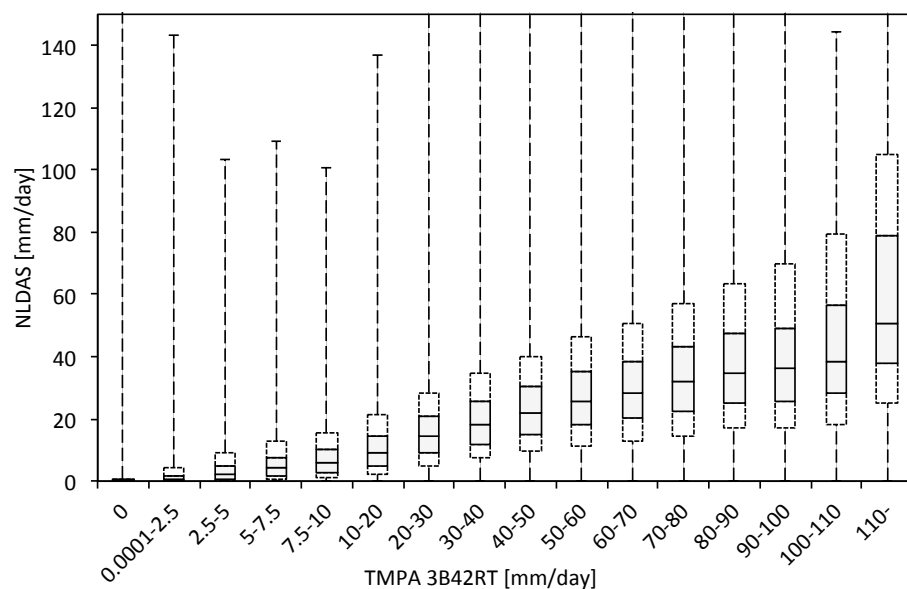
Authors 8/31/2015 3:38 PM

Deleted: Page Break

... [337]

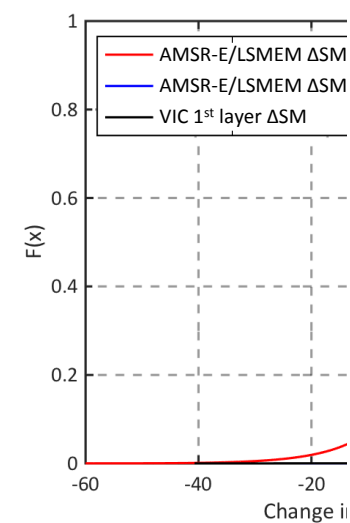


Authors 8/31/2015 3:38 PM  
 Deleted: handling  
 Authors 8/31/2015 3:38 PM  
 Deleted: density handling strategy  
 Authors 8/31/2015 3:38 PM  
 Deleted: Page Break  
 ... [338]



Authors 8/31/2015 3:38 PM

Deleted: Page Break



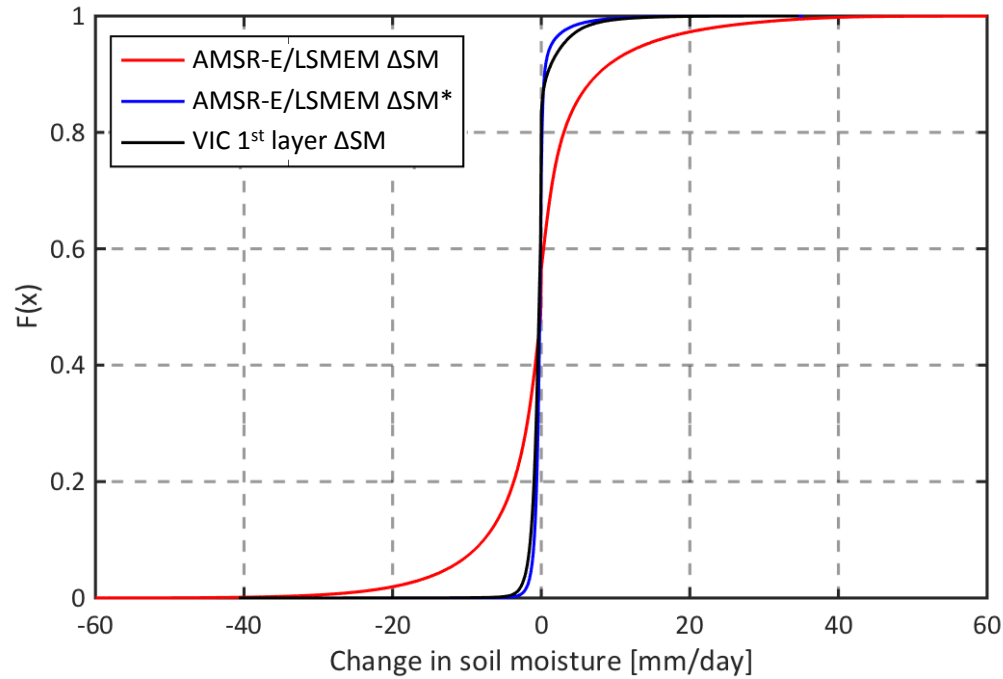


Figure 4 Empirical cumulative distribution function of changes in soil moisture from top layer soil moisture from NLDAS precipitation forced VIC simulation (black), and AMSR-E/LSMEM soil moisture retrieval before (red) and after (blue) pre-processing.

Authors 8/31/2015 3:38 PM

Deleted: Page Break

... [339]

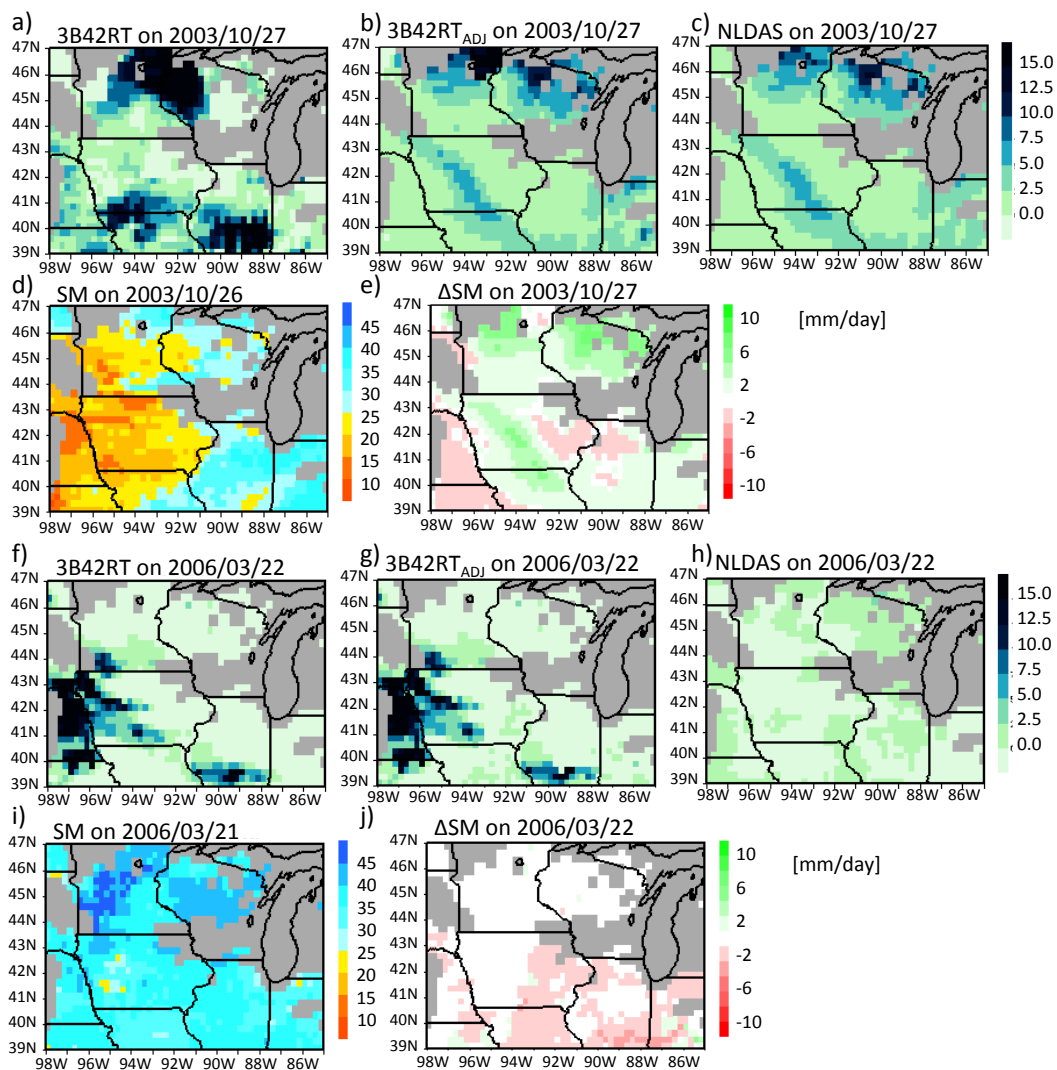


Figure 5 Two cases with recovered spatial rainfall pattern in the idealized experiment after merging satellite soil moisture retrieval on: (a-e) 27<sup>th</sup> Oct. 2003 and (f-j) 22<sup>th</sup> Mar. 2006.

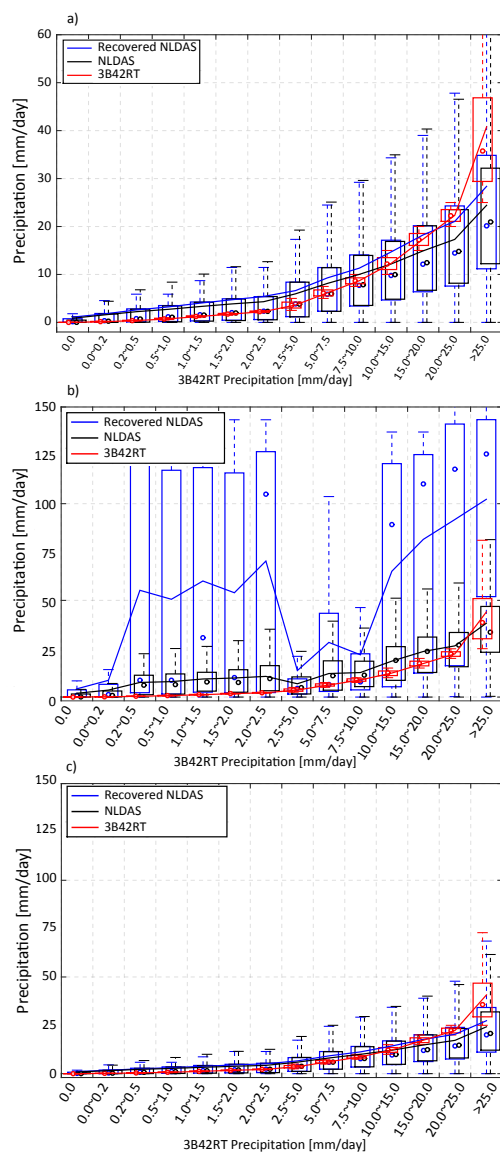
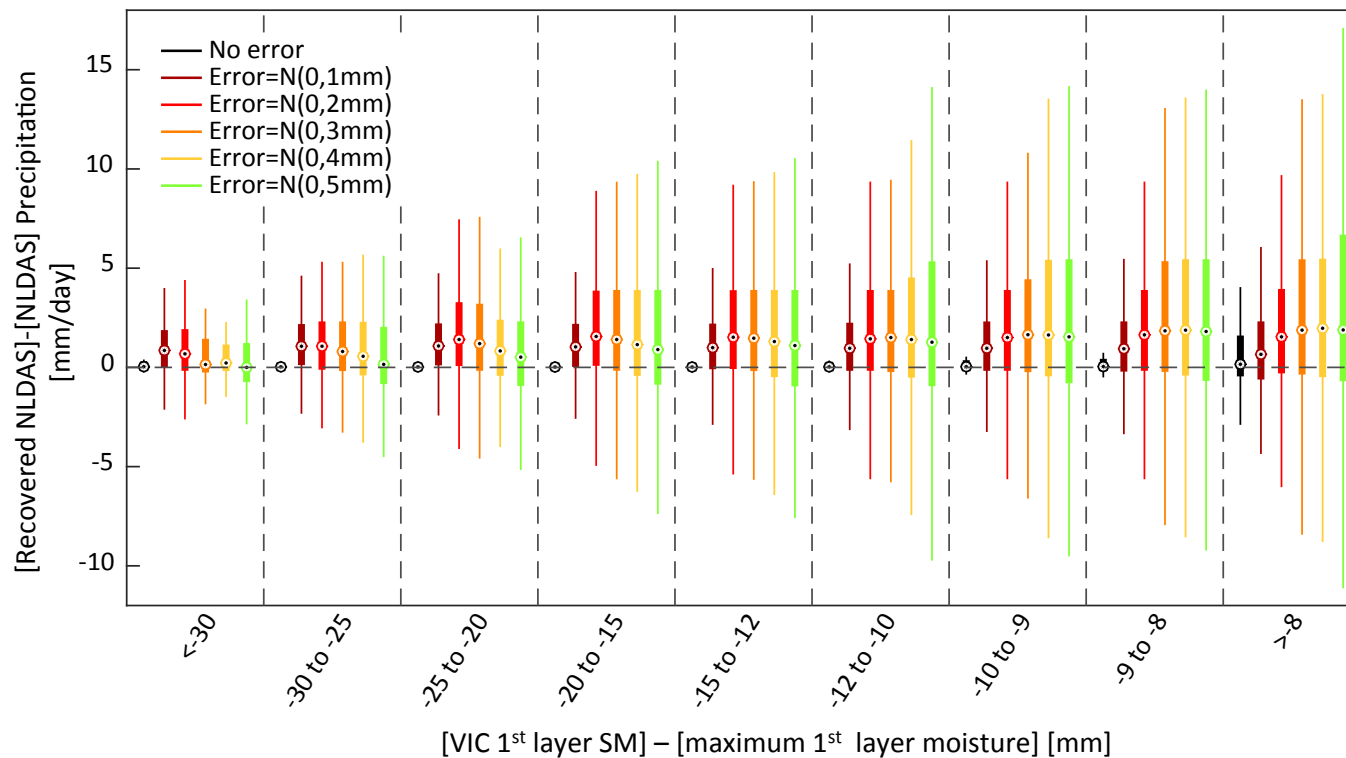


Figure 6 Accuracy of recovered precipitation in idealized experiment: (a) overall performance and separately comparing the improvement performance of recovered NLDAS precipitation (b) with and (c) without surface saturation condition. Statistics provided in Table 1.





Authors 8/31/2015 3:38 PM  
**Formatted:** Left

Authors 8/31/2015 3:38 PM  
**Deleted:** .5mm

Authors 8/31/2015 3:38 PM  
**Deleted:** 1.0mm

Authors 8/31/2015 3:38 PM  
**Deleted:** 1.5mm), N(0,2.0mm), N(0,2.5mm), N(0,3.0mm), N(0,3.5mm), N(0,4.0mm), N(0,4.5mm

Authors 8/31/2015 3:38 PM  
**Deleted:** 5.0mm

Authors 8/31/2015 3:38 PM  
**Deleted:** [Page Break](#)

a)  $\Delta SM$

b) 3B42

Figure 7 Error in recovered NLDAS precipitation given surface moisture condition. Recovered NLDAS is based on using “truth” soil moisture and soil moisture with normal error:  $N(0,1mm)$ ,  $N(0,2mm)$ ,  $N(0,3mm)$ ,  $N(0,4mm)$  and  $N(0,5mm)$ . Statistics provided in Table 2.

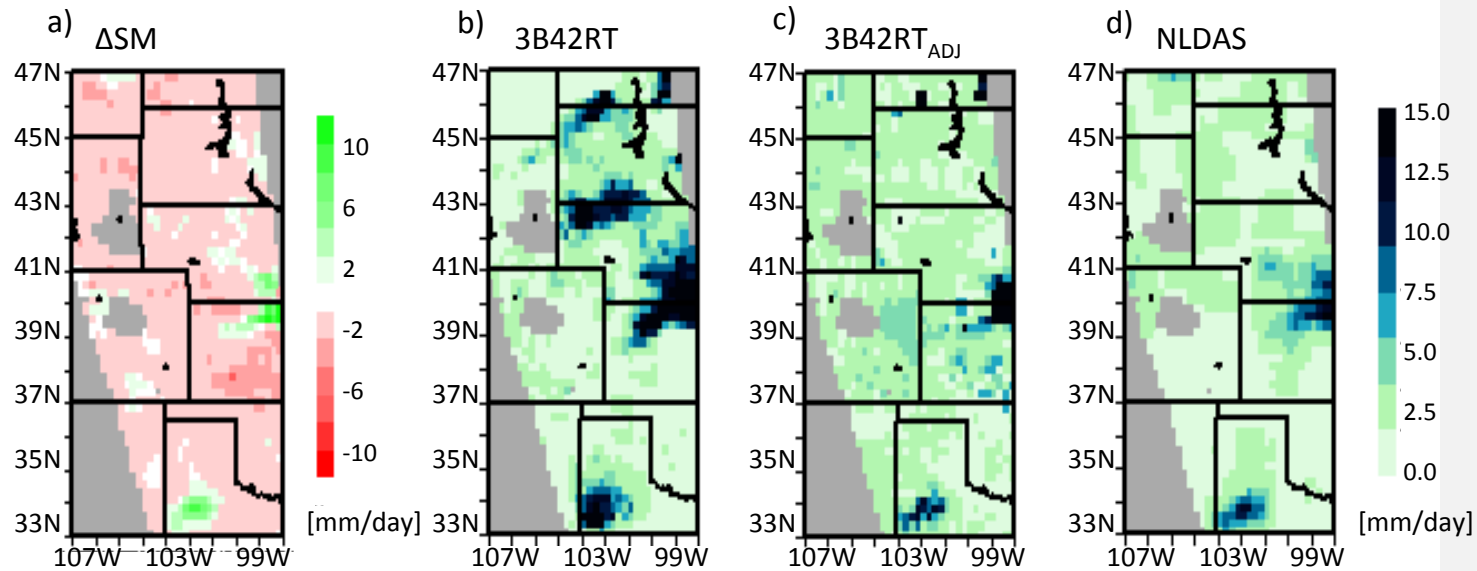


Figure 8 May 26<sup>th</sup> 2006 Rainfall pattern in 3B42RT (b) against NLDAS (d) as detected by AMSR-E/LSMEM  $\Delta SM$  (a), and recovered rainfall field (3B42RT<sub>ADJ</sub>) by assimilating AMSR-E/LSMEM  $\Delta SM$  (c). Gray shading shows area without soil moisture retrievals.

Authors 8/31/2015 3:38 PM

Deleted: into TMPA

Authors 8/31/2015 3:38 PM

Deleted: Page Break

... [341]

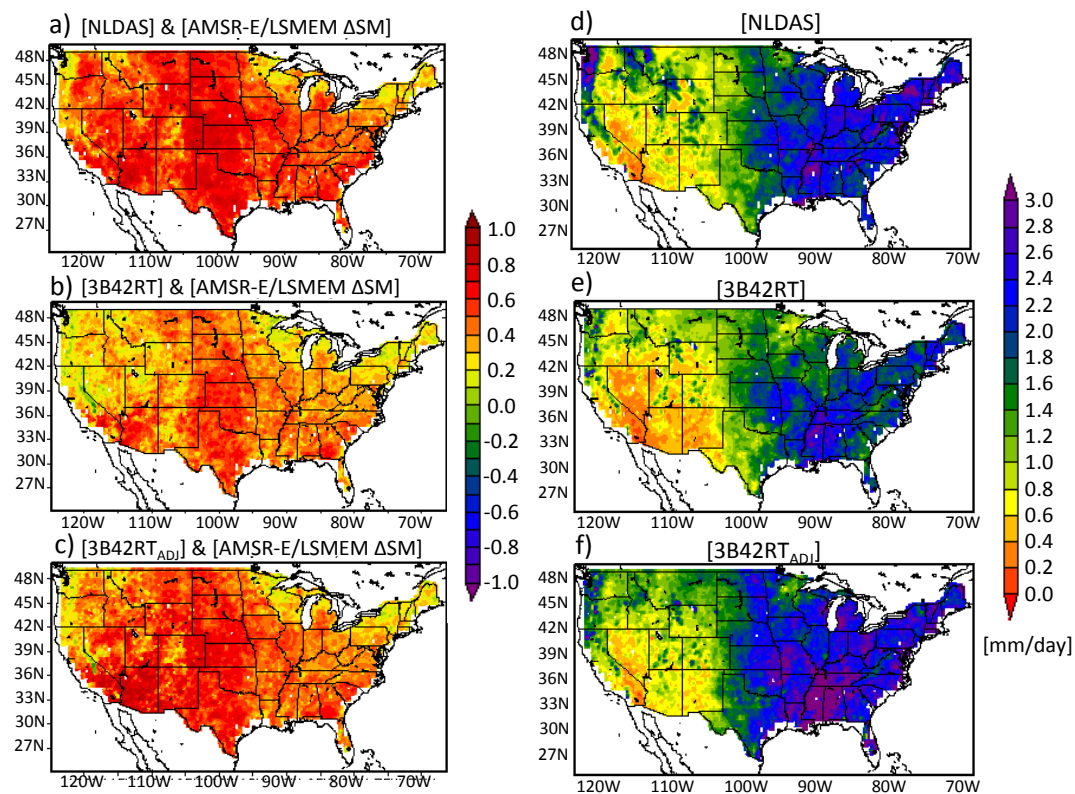


Figure 9 Pearson correlation coefficient between AMSR-E/LSMEM  $\Delta$ SM and precipitation: a) NLDAS, b) 3B42RT and c) 3B42RT<sub>ADJ</sub>; annual mean precipitation in d) NLDAS, e) 3B42RT and f) 3B42RT<sub>ADJ</sub> of time steps with AMSR-E/LSMEM  $\Delta$ SM retrievals.

Authors 8/31/2015 3:38 PM

**Deleted:** FAR, POD

Authors 8/31/2015 3:38 PM

**Deleted:** frequency of rainy days

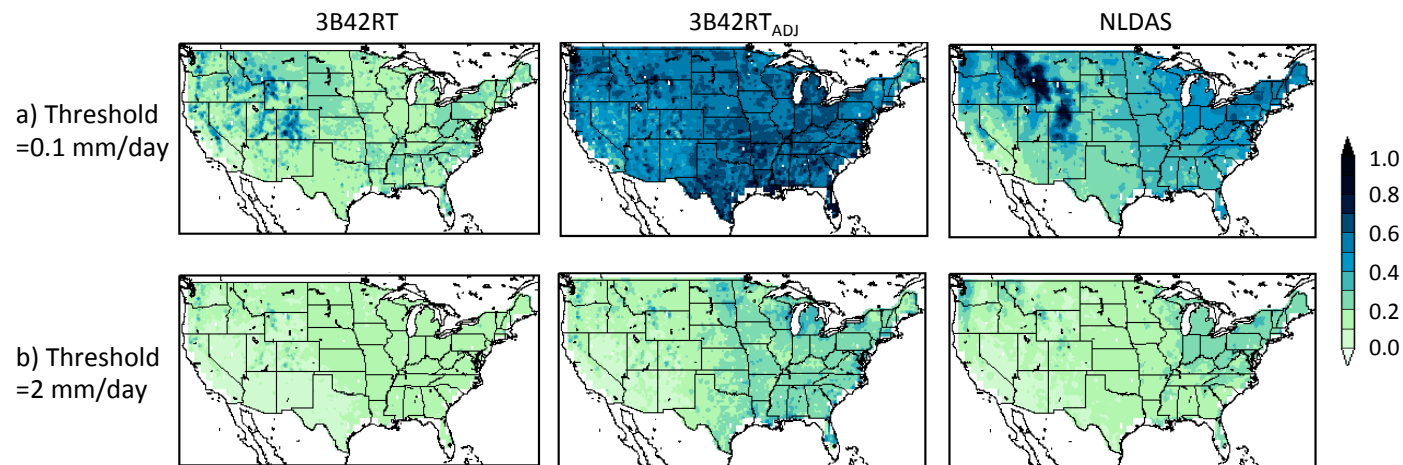


Figure 10 Frequency of rainy days in 3B42RT, 3B42RT<sub>ADJ</sub> and NLDAS with a) 0.1 mm/day and b) 2 mm/day rainfall threshold to define a rain day.

Authors 8/31/2015 3:38 PM

Deleted: 1mm

Authors 8/31/2015 3:38 PM

Deleted: (top)

Authors 8/31/2015 3:38 PM

Deleted: 2mm

Authors 8/31/2015 3:38 PM

Deleted: (bottom)

Authors 8/31/2015 3:38 PM

Deleted: event

Authors 8/31/2015 3:38 PM

Deleted: .

... [342]

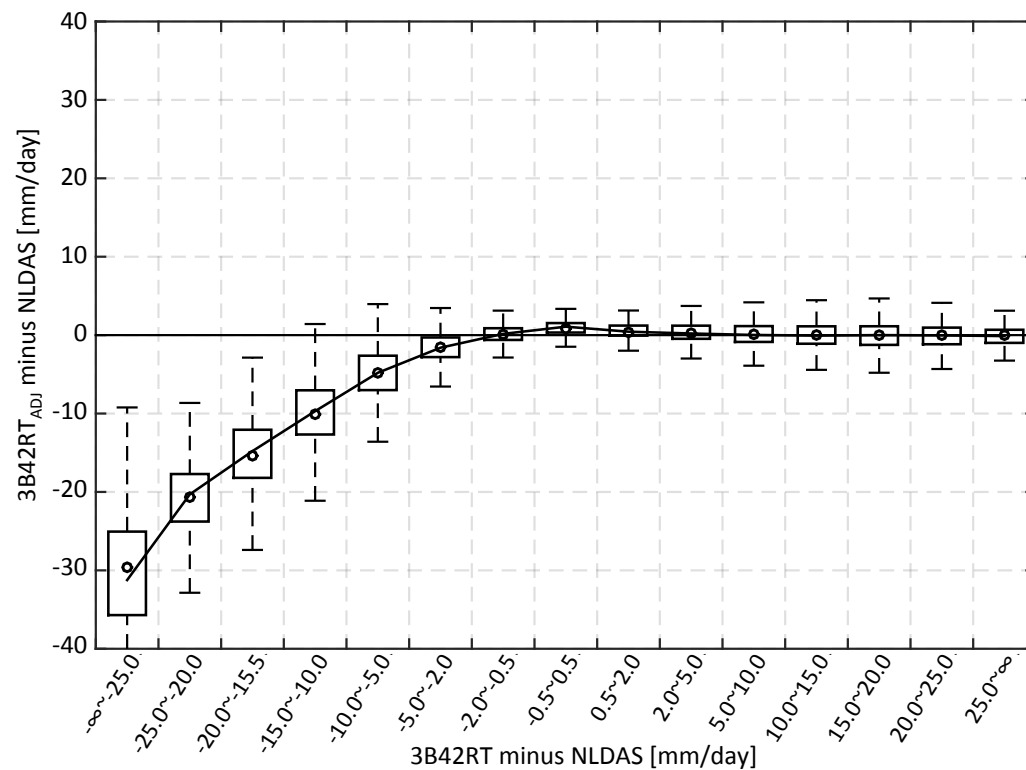


Figure 11 Distribution of 3B42RT and 3B42RT<sub>ADJ</sub> precipitation error compared to NLDAS. Statistics are provided in Table 3.

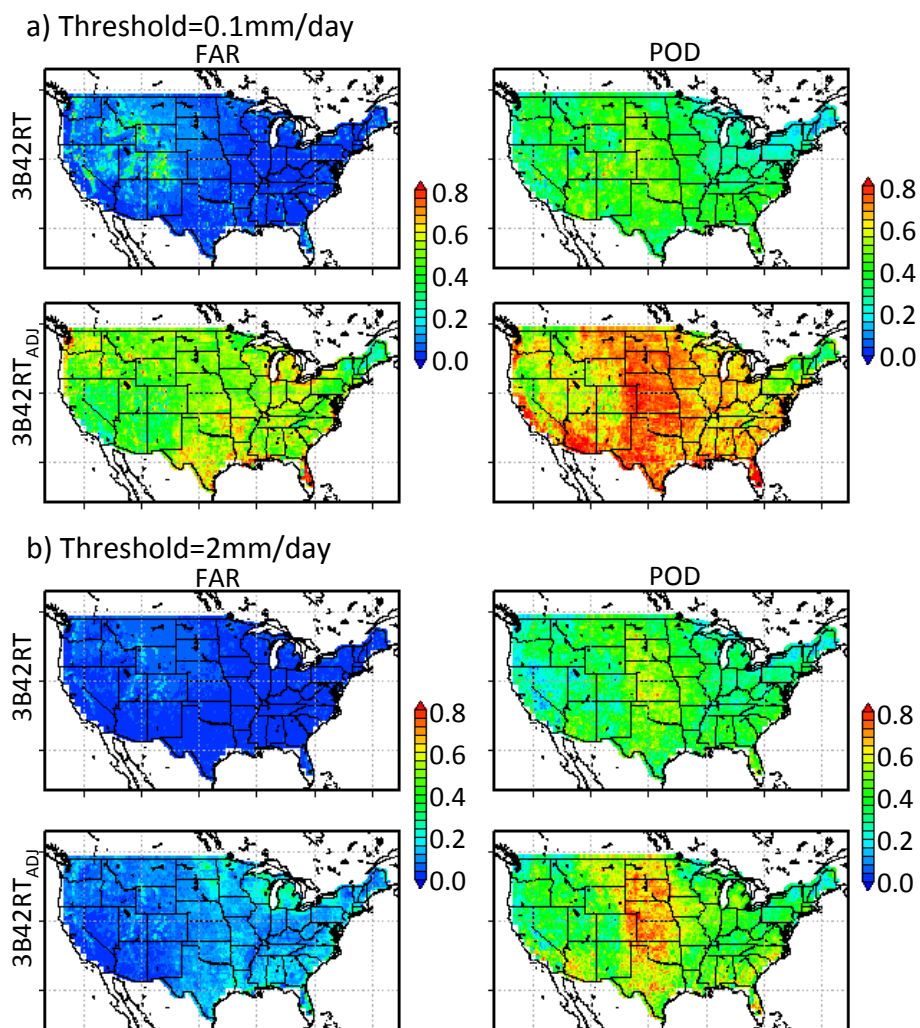


Figure 12 FAR and POD of 3B42RT and 3B42RT<sub>ADJ</sub> with a) 0.1 mm/day and b) 2 mm/day rainfall threshold to define a rain event.

Authors 8/31/2015 3:38 PM

**Deleted:** (a-b) Difference in mean absolute error

Authors 8/31/2015 3:38 PM

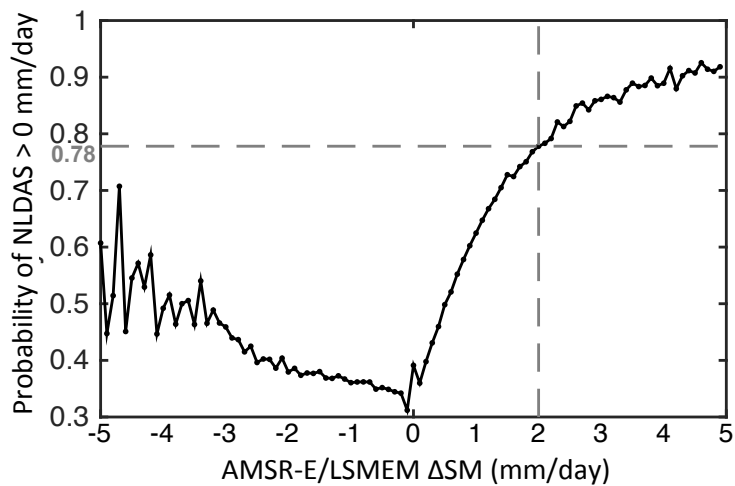
**Deleted:** and 3B42RT compared to NLDAS (MAE(3B42RT<sub>ADJ</sub>)-MAE(3B42RT)); (c-d) same as (a-b), after 2mm

Authors 8/31/2015 3:38 PM

**Deleted:** cutoff ΔSM

Authors 8/31/2015 3:38 PM

**Deleted:** is applied



Authors 8/31/2015 3:38 PM

Deleted: Page Break

... [344]

Authors 8/31/2015 3:38 PM

Deleted: Distribution of

Authors 8/31/2015 3:38 PM

Deleted: when rainy days are added in 3B42RT<sub>ADJ</sub> (no rain in 3B42RT, rain in 3B42RT<sub>ADJ</sub>)

Authors 8/31/2015 3:38 PM

Deleted: .

... [345]

Figure 13 Probability that the added rainy days ( $3B42RT = 0$  mm/day,  $3B42RT_{ADJ} > 0$  mm/day) are true rain events ( $NLDAS > 0$  mm/day) given corresponding AMSR-E/LSMEM  $\Delta SM$ .